

NATIONAL BUREAU OF STANDARDS
MICROCOPY RESOLUTION TEST CHART

①

AD-A157 973

SQUALL AND CLOUD LINES AS
STRUCTURAL COMPONENTS OF AN
ARABIAN SEA CONVECTIVE CLOUD CLUSTER

Charles Loren Benson, Jr., B. S.

DTIC
SELECTED
AUG 16 1985
S D

DTIC FILE COPY

A Thesis Presented to the Faculty of the Graduate School
of Saint Louis University in Partial Fulfillment of
the Requirements for the Degree of
Master of Science (Research)

1985

This document has been approved
for public release and sale; its
distribution is unlimited.

UNCLASS

SECURITY CLASSIFICATION OF THIS PAGE (When Data Entered)

REPORT DOCUMENTATION PAGE		READ INSTRUCTIONS BEFORE COMPLETING FORM
1. REPORT NUMBER AFIT/CI/NR 85-83T	2. GOVT ACCESSION NO.	3. RECIPIENT'S CATALOG NUMBER
4. TITLE (and Subtitle) Squall and Cloud Lines as Structural Components of an Arabian Sea Convective Cloud Cluster		5. TYPE OF REPORT & PERIOD COVERED THESIS/DISSEMINATION
		6. PERFORMING ORG. REPORT NUMBER
7. AUTHOR(s) Charles Loren Benson, Jr.		8. CONTRACT OR GRANT NUMBER(s)
9. PERFORMING ORGANIZATION NAME AND ADDRESS AFIT STUDENT AT: Saint Louis University		10. PROGRAM ELEMENT, PROJECT, TASK AREA & WORK UNIT NUMBERS
11. CONTROLLING OFFICE NAME AND ADDRESS AFIT/NR WPAFB OH 45433		12. REPORT DATE 1985
		13. NUMBER OF PAGES 96
14. MONITORING AGENCY NAME & ADDRESS (if different from Controlling Office)		15. SECURITY CLASS. (of this report) UNCLASS
		15a. DECLASSIFICATION/DOWNGRADING SCHEDULE
16. DISTRIBUTION STATEMENT (of this Report) APPROVED FOR PUBLIC RELEASE; DISTRIBUTION UNLIMITED		
17. DISTRIBUTION STATEMENT (of the abstract entered in Block 20, if different from Report)		
18. SUPPLEMENTARY NOTES APPROVED FOR PUBLIC RELEASE: IAW AFR 190-1		<i>Lynn E. Wolaver</i> LYNN E. WOLAVER Dean for Research and Professional Development SAUG 1985 - AFIT, Wright-Patterson AFB OH
19. KEY WORDS (Continue on reverse side if necessary and identify by block number)		
20. ABSTRACT (Continue on reverse side if necessary and identify by block number) ATTACHED		

DD FORM 1 JAN 73 1473

EDITION OF 1 NOV 65 IS OBSOLETE

UNCLASS

85 8 13 080

SECURITY CLASSIFICATION OF THIS PAGE (When Data Entered)

AFIT RESEARCH ASSESSMENT

The purpose of this questionnaire is to ascertain the value and/or contribution of research accomplished by students or faculty of the Air Force Institute of Technology (AU). It would be greatly appreciated if you would complete the following questionnaire and return it to:

AFIT/NR
Wright-Patterson AFB OH 45433

RESEARCH TITLE: Squall and Cloud Lines as Structural Components of an Arabian
Sea Convective Cloud Cluster

AUTHOR: Charles Loren Benson, Jr.

RESEARCH ASSESSMENT QUESTIONS:

1. Did this research contribute to a current Air Force project?

a. YES

b. NO

2. Do you believe this research topic is significant enough that it would have been researched (or contracted) by your organization or another agency if AFIT had not?

a. YES

b. NO

3. The benefits of AFIT research can often be expressed by the equivalent value that your agency achieved/received by virtue of AFIT performing the research. Can you estimate what this research would have cost if it had been accomplished under contract or if it had been done in-house in terms of manpower and/or dollars?

a. MAN-YEARS _____

b. \$ _____

4. Often it is not possible to attach equivalent dollar values to research, although the results of the research may, in fact, be important. Whether or not you were able to establish an equivalent value for this research (3. above), what is your estimate of its significance?

a. HIGHLY
SIGNIFICANT

b. SIGNIFICANT

c. SLIGHTLY
SIGNIFICANT

d. OF NO
SIGNIFICANCE

5. AFIT welcomes any further comments you may have on the above questions, or any additional details concerning the current application, future potential, or other value of this research. Please use the bottom part of this questionnaire for your statement(s).

NAME _____

GRADE _____

POSITION _____

ORGANIZATION _____

LOCATION _____

STATEMENT(s):

FOLD DOWN ON OUTSIDE - SEAL WITH TAPE

AFIT/NR
WRIGHT-PATTERSON AFB OH 45433
OFFICIAL BUSINESS
PENALTY FOR PRIVATE USE, \$300



NO POSTAGE
NECESSARY
IF MAILED
IN THE
UNITED STATES

BUSINESS REPLY MAIL
FIRST CLASS PERMIT NO. 73236 WASHINGTON D.C.

POSTAGE WILL BE PAID BY ADDRESSEE

AFIT/ DAA
Wright-Patterson AFB OH 45433



FOLD IN

DIGEST

This research has several objectives. First, it attempts to present a description of the kinematic, thermal, and cloud structure of an eastern Arabian Sea convective cloud cluster. Secondly, this research will determine the horizontal location of updrafts, downdrafts, and gust fronts in relation to observed convection. The last objective is to determine the extent of boundary layer modification by convection. Although this last objective has been accomplished in the tropical Atlantic and Pacific Oceans, it has never been attempted over the Arabian Sea.

During the Monsoon Experiment 1979 (MONEX-79), a unique mix of meteorological data was obtained on 20 June 1979 to observe a convective cloud cluster that formed over the extreme eastern Arabian Sea. The data used in this research consisted of rawinsonde data from India's mainland and island stations, research ship data, research aircraft data, and satellite data.

Careful study of all available data revealed several squall lines (as well as other types of convection) embedded in the larger scale cloud cluster. The squall lines were found to form and decay as a result of complex interactions between synoptic scale features (i.e., the Tropical Easterly Jet and the Somalia low-level jet), mesoscale features (i.e., mesoscale wind speed

variability and mesoscale downdrafts), and convective-scale features (convective scale updrafts and downdrafts).

Numerous differences were observed between the squall lines examined in this study and squall lines observed during the Global Atmospheric Research Program's Atlantic Tropical Experiments (GATE). The main differences include: Arabian Sea squall lines were quasi-stationary, while GATE squall lines were moving; Arabian Sea squall lines existed in a more highly sheared environment than GATE convection; the low-level inflow air in Arabian Sea squall lines could be influenced by subsidence from a trailing anvil cloud, while GATE convection's low-level inflow generally was not.

This thesis shows conclusively that boundary layer influences caused by convection over the Arabian Sea must be considered when attempting to describe (either qualitatively or numerically) Indian southwest monsoonal rainfall.

ACKNOWLEDGEMENTS

I am deeply grateful to my advisor, Dr. G. V. Rao, for his unswerving support and encouragement. His constant availability for discussions made the exchange of new ideas concerning this research very easy. I am also appreciative of the constructive comments made by the other two members of my committee, Dr. Albert J. Pallmann and Dr. James T. Moore.

Dr. Rod Scofield (National Weather Service) took time out of his busy schedule to make constructive remarks regarding satellite observed cloud features studied in this research. Dr. Hsiao-Ming Hsu (NCAR)* did the same during his recent visit to Saint Louis University. Mr. Chia-wei Tao aided in formulating computer programs used in this study. Mr. Eric Haug (Saint Louis University) and Dr. Dale Meyer (Air Weather Service) were instrumental in extracting usable data from the Electra aircraft's gust probe tapes.

I am indebted to my wife, Lisa Anne Benson, for her patience and support during the many long hours I spent on this research. I sincerely thank Ms. Rhonda Webb for her professional and positive attitude in the typing of this manuscript (that included many revisions). Without her hard work it is doubtful that this

*National Center for Atmospheric Research, sponsored by the National Science Foundation.

research could have been completed nearly so quickly.

I am thankful that the United States Air Force gave me the opportunity to attend Saint Louis University and complete the program requirements.

This research was sponsored by the National Science Foundation (NSF) under Grant ATM 83-12517.

TABLE OF CONTENTS

	Page
ACKNOWLEDGEMENTS	iii
TABLE OF CONTENTS	v
LIST OF TABLES	vii
LIST OF FIGURES	viii
1. INTRODUCTION	1
a. <u>Motivation for study</u>	1
b. <u>Historical perspective</u>	2
c. <u>Research objectives</u>	9
d. <u>Research methodology</u>	10
2. DATA SOURCES	14
a. <u>Upper-air data</u>	14
b. <u>Dropwindsonde (DWS) data</u>	14
c. <u>Descent and ascent sounding data</u>	16
d. <u>Electra fast-response data</u>	18
e. <u>Other Electra data</u>	18
f. <u>AVRO data</u>	20
g. <u>Surface data</u>	22
h. <u>Satellite data</u>	22
i. <u>Radar data</u>	23
j. <u>Other data sources</u>	23

TABLE OF CONTENTS (CONTINUED)

	Page
3. THE "PARENT" CONVECTIVE CLOUD CLUSTER	25
a. <u>Satellite observed life history</u>	25
b. <u>Kinematic fields</u>	31
c. <u>Divergence fields</u>	36
d. <u>Thermodynamic considerations</u>	41
4. COMPONENT CONVECTION	48
a. <u>Mesoscale blob profile</u>	48
b. <u>Squall line profile</u>	52
c. <u>Thunderstorm profile</u>	65
d. <u>Squall line influences at Amini</u>	69
e. <u>Measured vertical velocity events</u>	73
5. SUMMARY AND CONCLUSIONS	80
a. <u>Summary of research</u>	81
b. <u>Arabian Sea vs. GATE convection</u>	84
c. <u>Conclusions</u>	88
APPENDIX	90
BIBLIOGRAPHY	92
VITA AUCTORIS	96

LIST OF TABLES

Table		Page
1	Surface weather elements observed at Amini on 20 June 1979	72
2	Updraft data as measured by the Electra's gust probe from 0447-0517 GMT on 20 June 1979	77
3	Same as Table 2, but for downdraft measurements ...	78

LIST OF FIGURES

Figure		Page
1	Upper-air observational network used in the 20 June 1979 analysis	15
2	Dropwindsonde (DWS) release points from the Electra aircraft on 20 June 1979	17
3	Flight path of the Electra on 20 June 1979	19
4	Flight path of India's AVRO research aircraft on 20 June 1979	21
5	GOES-I infrared imagery for 20 June 1979: 0000 GMT (top), 0600 GMT (bottom)	26
6	GOES-I visual imagery for 20 June 1979: 0900 GMT (top), 1200 GMT (bottom)	27
7	GOES-I infrared imagery for 20 June 1979: 1200 GMT (top), 1500 GMT (bottom)	29
8	GOES-I infrared imagery for 20 June 1979: 1800 GMT (top), 2300 GMT (bottom)	30
9	Surface pressure analysis for 1200 GMT 20 June 1979	32
10	900 mb winds ($m s^{-1}$) for 1200 GMT 20 June 1979 ...	34
11	900 mb winds ($m s^{-1}$) for 0600 GMT 20 June 1979 ...	35
12	500 mb winds ($m s^{-1}$) for 1200 GMT 20 June 1979 ...	37
13	200 mb winds ($m s^{-1}$) for 1200 GMT 20 June 1979 ...	38
14	Computed 850 mb divergence ($\times 10^{-5} s^{-1}$) field for 1200 GMT 20 June 1979	40
15	Computed 200 mb divergence ($\times 10^{-5} s^{-1}$) field for 1200 GMT 20 June 1979	42
16	Computed profiles of virtual potential temperature (θ_v) for ship Deepak (0600 GMT) and DWS #3 (0524 GMT) on 20 June 1979	44

LIST OF FIGURES (CONTINUED)

		Page
17	Computed profiles of wet-bulb potential temperature (θ_w) for ship Deepak (0600 GMT) and DWS #3 (0524 GMT) on 20 June 1979	46
18	UWSSEC's nephanalysis for 0600 GMT 20 June 1979 .	49
19	Computed profiles of wet-bulb potential temperature (θ_w) for DWS #2 (0449 GMT) and DWS #3 (0524 GMT) on 20 June 1979	50
20	Electra cloud camera photo (right side) for 0526 GMT 20 June 1979	53
21	Electra cloud camera photo (left side) for 0526 GMT 20 June 1979	53
22	Schematic of Electra descent sounding	55
23	Cloud camera photo (right side) for 0530 GMT 20 June 1979	56
24	Computed profiles of wet-bulb potential temperature (θ_w) for DWS #3 (0524 GMT) and descent sounding for 20 June 1979	58
25	Computed profiles of virtual potential temperature (θ_v) for descent sounding and Zipser's idealized (1977) θ_v profile for 100-150 km behind a squall line	60
26	Temperature (solid) and dew point (dashed) traces for descent sounding	61
27	Electra upward looking Epply radiometer shortwave irradiance trace	64
28	Schematic of Electra ascent sounding	66
29	Computed profiles of wet-bulb potential temperature (θ_w) for DWS #3 (0524 GMT) and ascent sounding	67
30	Computed profiles of wet-bulb potential temperature (θ_w) for DWS #4 (0901 GMT) and ascent sounding on 20 June 1979	68
31	Computed profiles of wet-bulb potential temperature (θ_w) for station Amini (1200 GMT) and DWS #3 (0524 GMT) on 20 June 1979.....	71
32	GOES-I visual imagery for 0600 GMT 20 June 1979 ..	75

LIST OF FIGURES (CONTINUED)

		Page
33	Conceptual model (x-y plane) of the eastern Arabian Sea squall lines observed on 20 June 1979....	85
34	Conceptual model (y-z plane) of the eastern Arabian Sea squall observed on 20 June 1979	86

1. INTRODUCTION

a. Motivation for study

Tropical squall lines are important to meteorological research for several reasons. Squall lines supply substantial fractions of annual rainfall totals in the tropics. Houze (1977) reported that four squall lines accounted for 50% of the rainfall observed on one research ship during Phase 3 of the Global Atmospheric Research Program's Atlantic Tropical Experiment (GATE). A squall line to be described in this study deposited ~95 mm of rain during 20 June 1979 near 11.5°N, 74.0°E (Krishnamurti et al., 1983). Cases such as these strongly suggest that squall lines are an important component in the energy cycle of the tropical atmosphere.

Tropical squall lines are of the same temporal and spatial scales as spiral bands in tropical cyclones. A logical question is: what are the differences and/or similarities between tropical squall lines and spiral bands? An adequate resolution of this problem could answer many questions concerning tropical cyclone intensification from "seedling" convective cloud clusters.

Tropical squall lines are known to modify the atmospheric boundary layer during their passage. Essentially the boundary layer (BL) is stabilized after the squall passage inhibiting the development of new convection. For accurate numerical weather prediction (NWP) modeling of the tropical atmosphere, this BL

modification must be taken into account.

b. Historical perspective

Hamilton and Archbold (1945) gave the first discussion of tropical squall lines in the scientific literature. They described "disturbance lines" in their survey of Nigerian weather. The authors accurately depicted many of the salient features of tropical squall lines that are under study today. These features included:

- (1) A narrow zone of heavy rain that accompanies the arrival of the squall line.
- (2) A region of light stratiform rain falling from altostratus to the rear of the squall's leading edge.
- (3) A substantial drop in dry-bulb temperature as the squall line passes the station.
- (4) Mid-tropospheric air ahead of the squall line descending to the surface during squall passage. Surface air ahead of the squall is incorporated into active cumulonimbus towers, and rises to at least mid-tropospheric levels.

Zipser (1969) made the first serious attempt to analyze the effects of mesoscale downdrafts on the life cycle of a tropical disturbance. His study was made of a small disturbance that passed through the Line Islands in 1967. The tropical disturbance he studied strongly resembled a typical tropical squall

line. Zipser's analysis of satellite photos revealed that large portions of the cloud system were composed of relatively inactive stratiform cloud. Kinematic analysis showed that low-level convergence (probably responsible for initiating the convection) was confined to below the 950 mb level. Equivalent potential temperature (θ_e) profiles revealed that very low θ_e values near the surface were due to unsaturated descent of mid-tropospheric air to the lower troposphere. These low θ_e values were found in divergent flow in moderate to heavy rain falling from middle clouds. Zipser inferred that this area represented an area of mesoscale unsaturated downdraft generation. Cumulus development was inhibited in this region for some 6-12 hours, even though surface sensible and latent heat fluxes were positive and strong.

Quoting Zipser:

This air is therefore completely unable to take part in the deep convection required to maintain tropical disturbances, and in fact kills such convection everywhere that it spreads. (p. 813)

Betts, Grover, and Moncrief (1976) studied the characteristics of squall lines over Venezuela during the Venezuelan International Meteorological and Hydrological Experiment (VIMHEX-72). Squall line cloud top heights agreed well with moist adiabatic ascent from the sub-cloud layer. The authors concluded that squall lines over Venezuela (in general) transport sub-cloud layer air to the upper troposphere with insignificant mixing. As in Zipser's (1969) study, θ_e profiles were compared before and

after squall line passed. These profiles suggested that potentially-warm BL air had been transported to high levels; potentially colder mid-tropospheric air had descended to the BL.

Rao (1976) presented a comprehensive study of the Indian southwest monsoon. Rao pointed out that convection off India's west coast is often arranged in long bands parallel to the low-level flow. Convergence fields (on several scales) seemed to interact to intensify the convective bands. Rao noted that the understanding of the mesoscale features of these rain bands is far from complete.

Miller and Betts (1977) studied the characteristics of traveling "convective mesosystems" (including squall lines) using VIMHEX-72 data. The mesosystems were found to travel faster than the mean flow in which they were embedded. In each mesosystem studied, a net low-level cooling and drying of the sub-cloud layer was observed after the system passed. Miller and Betts contended that air descended from just above the pre-storm cloud base to cause the observed thermodynamic changes. The mesosystems seemed to have downdrafts of convective-scale and mesoscale origin. The convective-scale downdrafts were associated with the leading edge of the active convection in the mesosystem. The mesoscale downdrafts originated beneath the trailing anvil cloud in stratiform precipitation.

Zipser's classic paper (1977) described the role of convective-scale and mesoscale downdrafts as components of

tropical squall lines. The study was based on observations of a tropical squall line that passed through the Lesser Antilles in August of 1968. Using wet-bulb potential temperature (θ_w) profiles, Zipser concluded that convective-scale downdrafts (cool and nearly saturated) spread out from the bases of active convective towers comprising the leading edge of the squall line. These downdrafts occupied the lowest few hundred meters in the post-squall environment. Mesoscale downdrafts occurred in sinking from the base of a trailing, well-defined anvil cloud. Based on satellite data, the rear 80-90% of the squall line system was comprised of anvil cloud. Virtually all of the anvil cloud existed above the freezing level. The anvil cloud existed for several hours after the active convective towers had died. Very few low clouds existed beneath the anvil cloud. Zipser displayed soundings that showed the virtual disappearance of the mixed layer after squall passage. Mesoscale sinking beneath the anvil cloud was cited as a primary factor in the maintenance of a suppressed mixed layer.

Houze (1977) studied the structure and dynamics of a squall line that passed through the GATE area in September of 1974. Houze's idealized squall line cross-section strongly resembled Zipser's (1977). The salient features of the idealized cross-section were the narrow band (20-30 km wide) of intense convection along the leading edge of the squall, and the anvil cloud that trailed several hundred kilometers to the rear. Using

sounding data from the GATE ship array, lower θ_w air was found to replace high θ_w air at the surface after squall passage. This paralleled the findings by Zipser (1969, 1977). Houze found that nearly the entire horizontal area occupied by the squall line was characterized by convective-scale and mesoscale downdrafts. Houze also found that the precipitation from the trailing anvil cloud was not insignificant. He estimated 40% of the squall line precipitation fell from the trailing anvil cloud.

Leary and Houze (1979b) studied five cases of horizontally uniform precipitation falling in the rear of squall line systems during GATE. Using digitized radar data from GATE research ships, distinct bright bands were observed in all five cases. The bright bands were observed beneath the 0°C isotherm (near 4.5 km in height). The authors deduced that mesoscale ascent must be occurring above the base of the trailing anvil cloud. This was inferred from the anvil cloud's longevity, large dimensions, and the substantial rainfall rates. Moreover, they concluded precipitation evaporation from beneath the anvil cloud, coupled with cooling from melting at the anvil cloud base, can initiate and sustain downward motion. This downward motion maintains the mesoscale downdrafts in the rear of the squall-line system.

Fitzjarrald and Garstang (1981a) studied the planetary BL in and near the Intertropical Convergence Zone (ITCZ) during GATE. They stratified high resolution vertical sounding data into disturbed (precipitating convection modifying the BL via penetrative

downrafts) and undisturbed (fair weather cumulus with only an occasional weak radar echo) regimes. The authors found that as active precipitating convection passed over an observation site, the following changes in the BL occurred: (1) the surface temperature decreased, (2) the surface specific humidity decreased, and (3) the height of the mixed layer decreased dramatically. The mixed layer was observed to return to its normal depth some hours later. Fitzjarrald and Garstang classified BL modification by precipitating convection into three periods: (1) an initial cooling of the BL as the precipitating convection arrives, (2) a following period when the shallower and cooler mixed layer is maintained by downrafts, and (3) a final period when the mixed layer begins recovering to its normal depth in the "wake" of the storm.

Fitzjarrald and Garstang (1981b) modeled the recovery time of the mixed layer in the wake of GATE precipitating convection. They found that (theoretically) the mixed layer recovers much faster where surface winds were greater than 10 m s^{-1} . Long recovery times were restricted where surface winds were light ($<5 \text{ m s}^{-1}$). These theoretical results were substantiated by GATE observations of mixed layer recovery. Fitzjarrald and Garstang concluded that light winds in a wake area over a tropical ocean places a severe restriction on new convective development. The authors concluded by stating:

The limitation on the development of new moist convection would impose a space and time modulation on synoptic-

scale systems which may be crucial to the intensification or even survival of the synoptic-scale entity. (p. 1771)

Barnes and Garstang (1982) studied sub-cloud energetics in relation to GATE precipitation types and amounts. Results indicated that penetrative convective-scale downdrafts did not reach the surface unless precipitation was occurring. They also concluded that linearly shaped convective systems (i.e., squall lines) are the most efficient centers of energy exchange. Squall lines were cited as powerful vehicles for effecting energy exchange in the tropics.

Meyer (1982) was able to ascertain a distinct area of suppressed convective activity and another area of developing convecting activity over the eastern Arabian Sea in association with a 20 June 1979 convective cloud cluster. The suppressed area resembled a "wake area" behind a squall line (Johnson and Nicholls, 1983). This area was characterized by negative virtual heat fluxes in the lower BL. The area of developing convective activity resembled a "recovered" BL. This area was characterized by positive virtual heat fluxes in the lower BL. Meyer's work did not specifically address the relationship of the two areas to the distinct squall or cloud lines that comprised the convective cloud cluster.

Johnson and Nicholls (1983) prepared a composite BL relative to a squall moving through the GATE area on 12 September 1974 (Gamache and Houze, 1982). The shallowest mixed layer depths

coincided with a surface wind diffluence center beneath the precipitating anvil cloud (i.e., to the rear of the squall line's leading edge).

Grossman and Durran (1984) studied the effect of India's Western Ghat mountains as a mechanism for inducing deep convection over the Arabian Sea. Research flight data from 24 June 1979 found areas of suppressed convection just to the west of active cumulonimbi. Grossman and Durran hypothesized that the suppression of convection was due to downward motion beneath an extensive anvil cloud. This anvil was sheared to the west some 200 km from the area of active convection. The authors succinctly noted one major difference between this Indian Ocean convection and the GATE squall line studies: the high energy sub-cloud air over the Arabian Sea was pumped into the convection from beneath the trailing anvil (in GATE low energy sub-cloud air was under the trailing anvil).

a. Research objectives

The overwhelming majority of tropical squall line studies have been on systems in the tropical Atlantic and Pacific oceans. This should not imply that squall lines do not occur over the eastern Arabian Sea in association with India's southwest monsoon. Yet little work has been attempted in this area, and essentially this is an unexplored area of marine BL research. This study, using Monsoon Experiment 1979 (MONEX-79) data, will

examine the kinematic, thermal, and cloud structure of a convective cloud cluster that occurred on 20 June 1979 over the eastern Arabian Sea. It will present the updraft and downdraft strengths of this cloud system in the middle troposphere as disclosed by the Electra gust probe data. The existence of squall lines as components of the larger scale cloud cluster will be established. This study will discuss the horizontal location of the updrafts, downdrafts, and gustfronts in relation to the east-west oriented squall and cloud lines. Furthermore, this study will examine the eastern Arabian Sea BL modification by mesoscale squall lines and other convective entities.

d. Research methodology

This research seeks to meet the stated objectives through the careful integration of diverse data sources. These data sources include conventional rawinsonde and surface data from India's southwestern coastal and island stations. In addition, research ship data, research aircraft data (including high quality dropwindsonde data), and geosynchronous satellite imagery are used.

The ultimate goal of this research is to meet the stated objectives by a careful evaluation of the data at hand. Little quantitative information is known about eastern Arabian Sea convective cloud clusters and their component convection. A logical procedure is to present a phenomenological discussion of

observable characteristics of the synoptic scale convective cloud cluster. This is accomplished primarily through visual and infrared satellite imagery. Since squall lines are inherent to the cloud cluster under study, a phenomenological account of squall lines (and other component convection) is also presented. Such an account is possible utilizing satellite imagery, on-board scientists' notes from research aircraft, and cloud camera movies filmed from aboard one of the research aircraft.

Once a phenomenological description of the large scale cloud cluster and its component convection is complete, a conceptual framework of interactions on various meteorological scales will be forwarded. Clearly, this conceptualization, if correct, is the only way any computed numerical results will have any physical meaning. Conceptually, this research will describe a quasi-circular convective cloud cluster. This convective cloud cluster is composed of a number of convective entities, of which squall lines are the most important. Sinking air beneath a component squall line's precipitating anvil should inhibit new convective growth in some areas, while the outrush of cool, near-surface air (gust front) should enhance new convective growth in other areas. Synoptic scale influences by the Tropical Easterly Jet and the Somalia low-level jet may be of first order significance. Conceptually, the component squall lines (and other convective types) should radically alter the BL over the eastern Arabian Sea. This will be apparent through the scrutinization of

representative sounding data (conventional and dropwindsonde). Updrafts and downdrafts should be organized in preferred regions relative to component convection. These updrafts and downdrafts can be measured directly in the mid-troposphere from research aircraft. Also, inferences about updrafts and downdrafts can be made through thermodynamic tracing techniques.

Once a conceptual framework of the larger scale cloud cluster and its component convection has been established, this research will quantify these concepts through mathematization. For the large scale cloud cluster, this will be done by computing the divergence fields of the horizontal wind in the lower, middle, and upper-troposphere. This task is readily accomplished through analysis of the synoptic scale winds. BL modifications can be mathematized through derived thermodynamic parameters of the typical undisturbed environment being compared to those in an environment modified by precipitating convection. This is done by reducing rawinsonde and dropwindsonde data to profiles of a single thermodynamic variable (i.e., virtual potential temperature or wet-bulb potential temperature).

Finally, the calculated results are interpreted in light of phenomenological observations and conceptual ideas. The interpreted results will be forwarded as conclusions. The interpretation of this research's divergence fields may indicate that the large scale convective cloud cluster existed in a highly convergent BL flow. Interpretation of thermodynamic profiles may sug-

gest the BL flow actually gains energy as it flows west to east across the Arabian Sea. Interpretation of in-situ vertical velocity measurements and inferences from thermodynamic profiles may suggest convective-scale downdraft origin. Other calculations may suggest mesoscale sinking below the bases of thick anvil clouds associated with squall lines. Interpretation of BL measurements could suggest mixed layer depths are greatly reduced in the vicinity of precipitating convection, especially squall lines. This reduction in mixed layer depth becomes as important in governing new convective growth as synoptic scale forcing.

For accurate numerical modeling attempts of squall lines and cloud clusters over the eastern Arabian Sea, a first step is to obtain a firm physical understanding of the evolution of cloud clusters and their component convection. This research represents that first step.

2. DATA SOURCES

a. Upper-air data

The Indian rawinsonde network used for the 20 June 1979 analysis is shown in Fig. 1. Rawinsonde data were collected at 0000 and 1200 GMT at stations Bombay, Goa, Mangalore, and Cochin. Upper air data at 0000, 0600, 1200 and 1800 GMT were collected at stations Amini, Minicoy, and Trivandrum. Data from the research ship Deepak (15.0°N, 65.0°E) were available at 0600 and 1800 GMT. Rawinsonde data from these sources consisted of pressure (mb), height (gpm), temperature and dew point (°C), wind direction (deg), and wind speed (mps). Data levels above the surface were at 50 mb intervals, beginning at 1000 mb. Significant temperature levels were reported at all mainland and island stations. Significant wind and temperature levels were reported from the research ship Deepak. All upper air soundings from the radiosonde network were extracted from the MONEX-79 data manual (issued by the Indian Meteorological Department).

b. Dropwindsonde (DWS) data

NCAR's Electra research aircraft flew through the heart of the convective cloud cluster under study on 20 June. The Electra

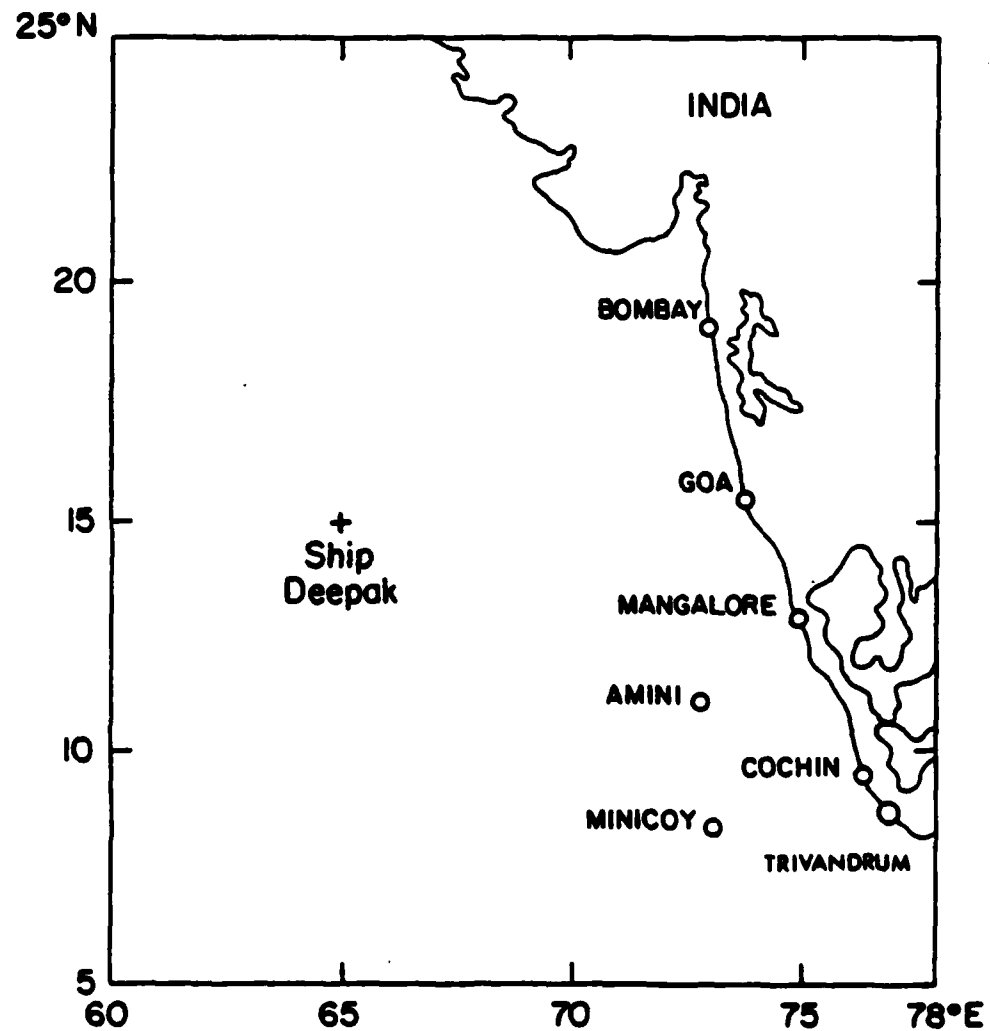


Fig. 1 Upper-air observational network used in the 20 June 1979 analysis.

released four DWS's in the analysis area that generated reliable data (data from a fifth DWS was judged erroneous shortly after its release). The DWS release points and times are shown in Fig. 2. Usually the first data level reported was just below flight level (this usually made the first data level around 510 mb). Standard levels reported were 700, 850, and 1000 mb. Significant wind and temperature levels were also reported. When mandatory and significant levels were plotted, data was available at about every 30 mb in the vertical. Temperature ($^{\circ}\text{C}$), dew point depression ($^{\circ}\text{C}$), wind direction (deg), and wind speed (mps) were reported at each data level. Specifics of dropwindsonde data acquisition and accuracy have been discussed by Bolhofer *et al.* (1981).

a. Descent and ascent sounding data

A descent sounding was made from the Electra during the period 0524-0544 GMT. Continuous measurements were made of pressure (mb), height (gpm), temperature and dew point ($^{\circ}\text{C}$), wind direction (deg), and wind speed (mps). These measurements were made as the Electra descended from 504 mb to begin its first set of BL measurements at ~ 100 m off the ocean surface.

An ascent sounding was made by the Electra from 0822-0842 GMT. Similar meteorological data as described for the descent sounding were recorded when the aircraft climbed from an altitude of ~ 100 m to about 575 mb. The ascent took place after the

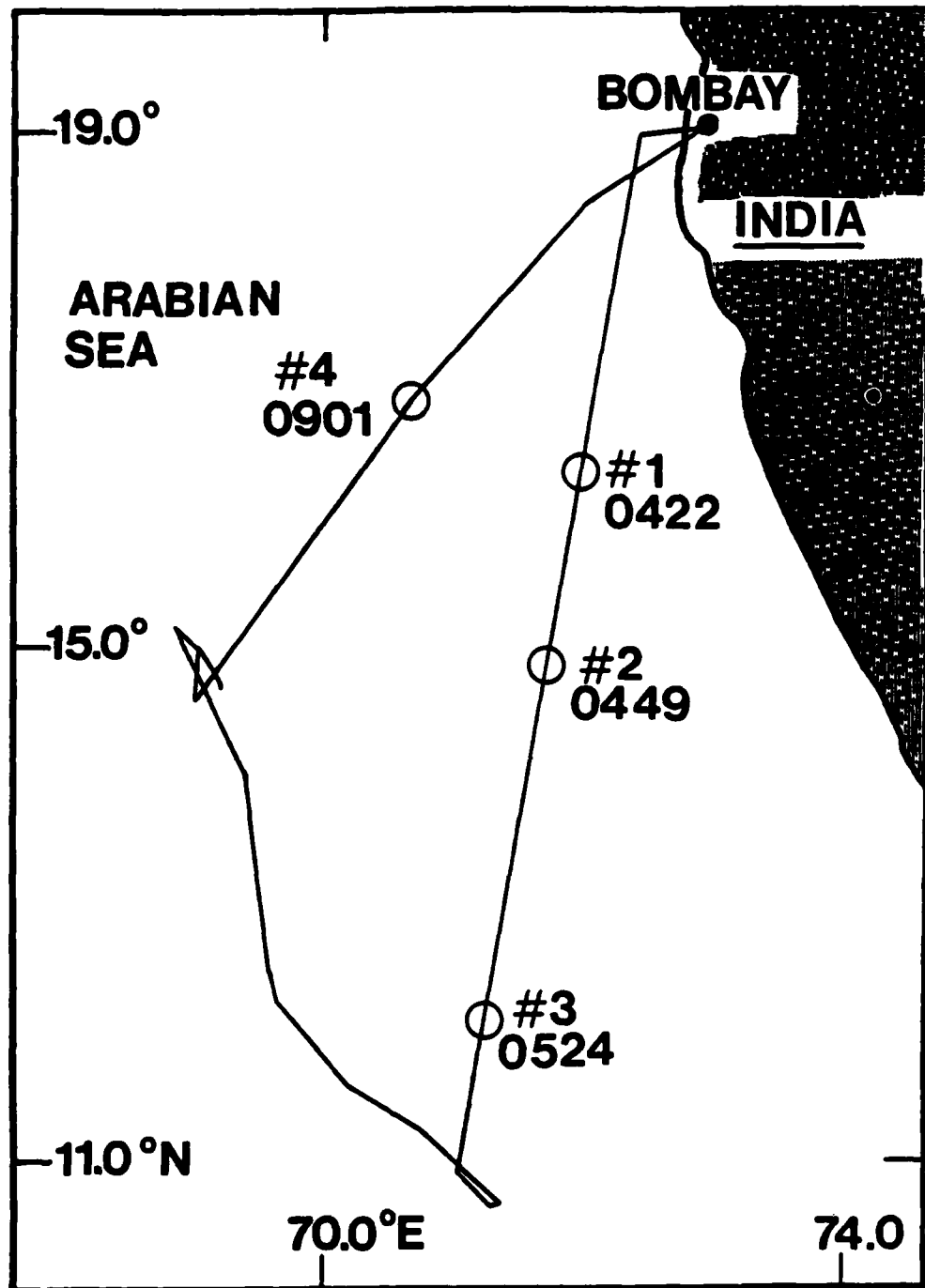


Fig. 2 Dropwindsonde (DWS) release points from the Electra aircraft on 20 June 1979. All times are in GMT.

aircraft completed a second set of BL measurements.

d. Electra fast-response data

A multitude of meteorological parameters were continuously recorded during the 20 June Electra research mission. Two sampling rates were used: 1 s^{-1} and 20 s^{-1} . The 20 s^{-1} data (fast response from the Electra gust probe) were used in this research primarily to study updrafts and downdrafts in the mid-troposphere. The fast response data were acquired in processed form on magnetic tapes from the NCAR. The specific parameters extracted from the processed data were ambient temperature, humidity, and vertical gust wind component. Details of the Electra's flight path are shown in Fig. 3.

e. Other Electra data

On board scientists' notes were obtained from the Electra's mission flight logs. The notes consisted of a series of visual observations and spot measurements of pressure (mb), temperature and dew point ($^{\circ}\text{C}$), wind directions (deg), and wind velocity (mps). The visual observations and spot measurements were recorded at irregular intervals, but were usually recorded every 4-5 minutes. The visual observations from the on board scientists were invaluable in reconstructing the sequence of weather events that transpired during the mission.

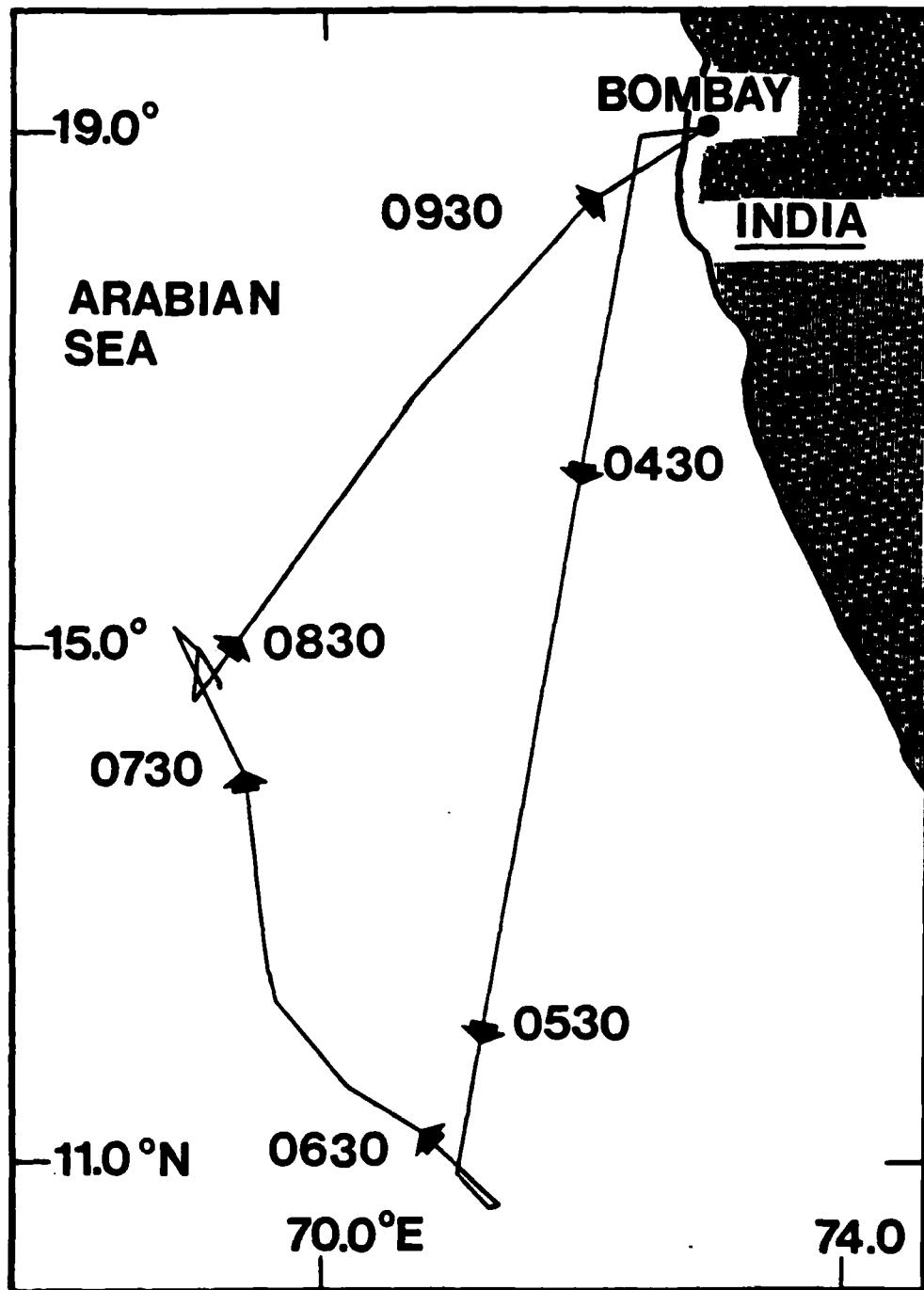


Fig. 3 Flight path of the Electra on 20 June 1979. All times are in GMT.

Upward looking Eppley radiometer measurements (1 s^{-1}) were also utilized in this study. These measurements were of shortwave infrared irradiance values (w m^{-2}). The measured values were read directly off microfilmed stripcharts.

Color 16 mm movies were obtained from the Electra's left side, right side, and downward looking cameras. These movies were viewed and analyzed with great care. Color prints were made from frames that showed notable cloud features during the mission.

f. AVRO data

The Indian government's AVRO aircraft performed a research mission into the convective cloud cluster from 0449-0939 GMT on 20 June. The aircraft's flight track is depicted in Fig. 4. The AVRO departed Bombay and flew at $\sim 836 \text{ mb}$ to 13.5°N , 70.5°E . Then the return leg to Bombay was flown at $\sim 692 \text{ mb}$. While tapes of raw data were not available from the AVRO mission, 2 minute spot measurements of temperature ($^{\circ}\text{C}$), wind direction (deg), and wind speed (knots) were recorded. A ascent profile of winds (836-400 mb) was executed near 14.0°N , 70.7°E . The aircraft then descended to $\sim 692 \text{ mb}$ for the return leg to Bombay. Logs of airborne scientists' notes were also available from the AVRO research mission. These logs were of great value in analyzing the sequence of events that transpired during the AVRO's mission.

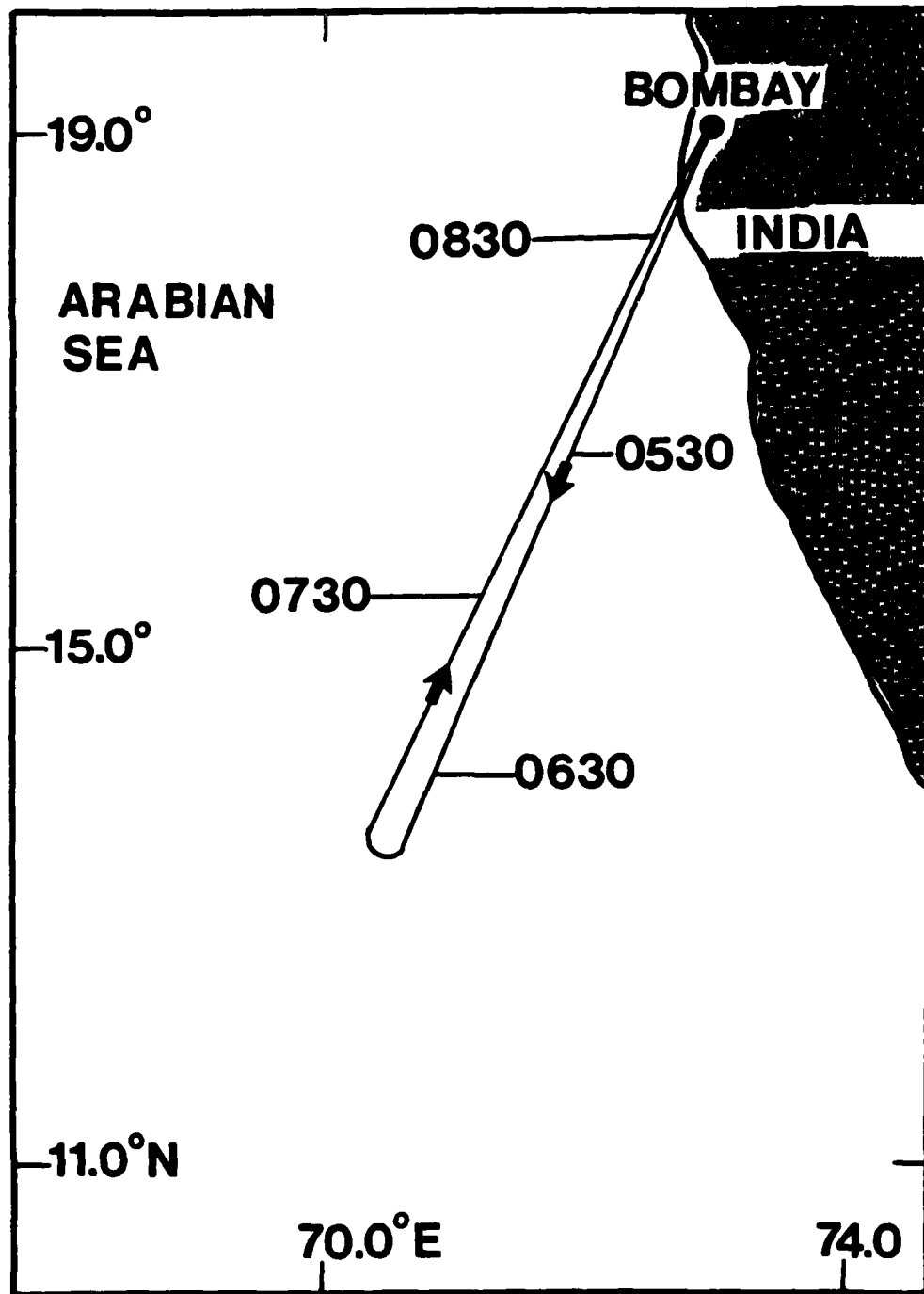


Fig. 4 Flight path of India's AVRO research aircraft on 20 June 1979. All times are in GMT.

g. Surface data

Surface observations at standard rawinsonde data times were available from the MONEX-79 data book. 3-hourly surface observations from stations along India's southwest coast were obtained from NCAR's data base. Some surface observations, a 0300 GMT surface analysis, and daily rainfall totals were obtained from the Indian Meteorological Department's Indian Daily Weather Report.

Several commercial ship surface observations were available over the eastern Arabian Sea on 20 June. These observations were contained in the Indian Daily Weather Report. All available commercial ship surface ship observations were used in surface analyses.

h. Satellite data

GOES-I satellite data for this study was obtained from the University of Wisconsin-Madison's Space Science and Engineering Center (UWSSEC). Data was available for 20 June at the following times: 0000 GMT (IR), 0600 GMT (visual and IR), 0900 GMT (visual and IR), 1200 GMT (visual and IR), and 1500, 1800, and 2300 GMT (IR). Resolution at satellite subpoint was 2.0 km for visual imagery, while infrared image resolution was 4.0 km. Scientists at the UWSSEC also supplied a detailed analysis of cloud types along the Electra's flight path.

i. Radar data

Copies of hourly radar images (PPI and RHI displays) from the Bombay radar installation were obtained. This 10 cm wavelength radar has a maximum operating range of 400 km in the PPI mode. The radar could only monitor the extreme northeastern portion of the convective cloud cluster on 20 June. But the radar data were useful in getting quantitative measurements of echo top heights, cell and line movements, etc. The RHI imagery was also useful in searching for indications of a bright band over the eastern Arabian Sea.

Unfortunately, no radarscope photos were available from either the Electra or AVRO aircraft. However, composite sketches of radar echoes observed during the Electra's flight were made by on board scientists. These sketches were utilized in this research.

i. Other data sources

The Quick Look (Krishnamurti et al., 1979) analysis of 850, 700 and 200 mb data was used to augment analysis over data-sparse areas (especially over the central Arabian Sea). Data from this source consisted of streamlines and isotachs for 1200 GMT for the 850, 700, and 200 mb levels.

Over-water precipitation estimates for 20 June were obtained from Precipitation Estimates from Raingauge and Satellite Obser-

vations Summer MONEX (Krishnamurti et al., 1983).

3. THE "PARENT" CONVECTIVE CLOUD CLUSTER

a. Satellite observed life history

GOES-I imagery revealed a disorganized mass of convection over the northeastern Arabian Sea as early as 19 June 1979. By 0000 GMT on 20 June, the system had consolidated into a convective cloud cluster just off India's west coast (Fig. 5). The more intense convection at this time appeared to be organized into a series of bands parallel to the low-level wind flow (which at this time was from the west-southwest). Rao (1976) recognized this banded feature of the Arabian Sea monsoonal convection in his detailed analysis of 1963 research flight data.

Visual satellite imagery at 0900 GMT (Fig. 6) shows the convective cloud cluster as it peaked in organization and concentration. The system at this time covered an area $\sim 1.2 \times 10^6$ km². Close examination of the 0900 GMT visual imagery shows an extensive cirrus shield covering the western 1/2 of the system. The cirrus is being blown towards the west by upper-level easterlies. This is a manifestation of the northern flank of the tropical easterly jet (TEJ). The strongest convection was occurring in the southeastern half of the cloud mass (mostly between 70-75°E and 10-15°N). As noted in 0000 GMT imagery, the 0900 GMT imagery

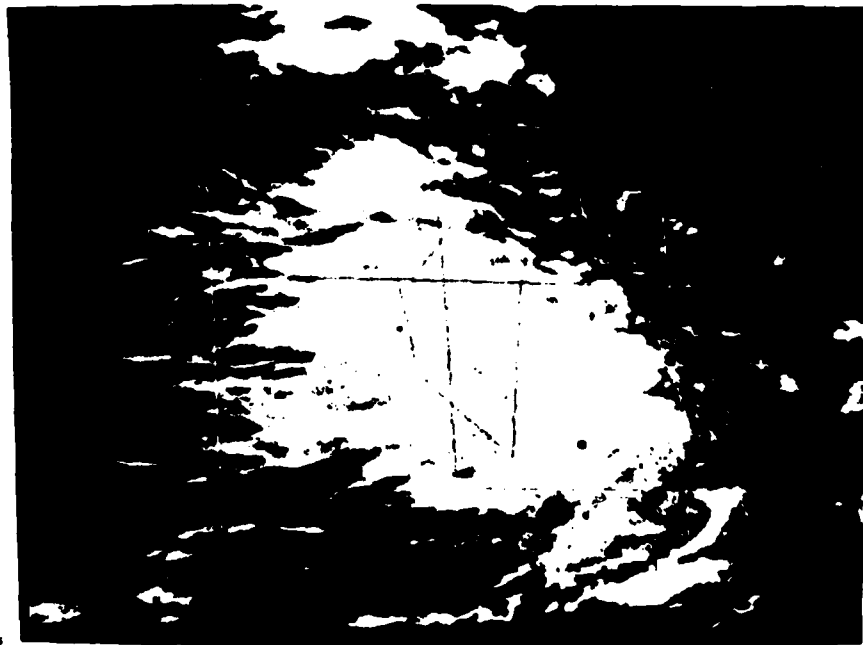
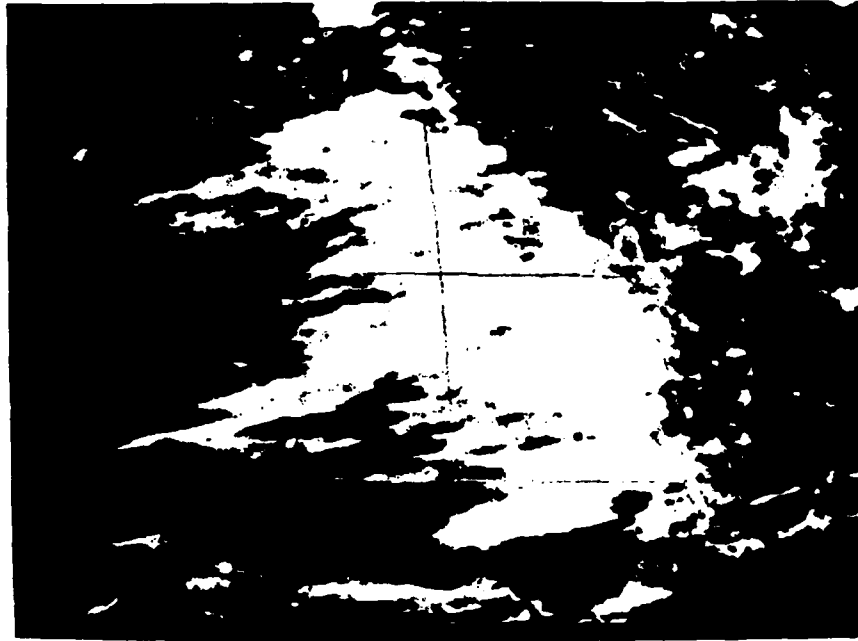


Fig. 5 GOES-I infrared imagery for 20 June 1979: 0000 GMT (top), 0600 GMT (bottom).

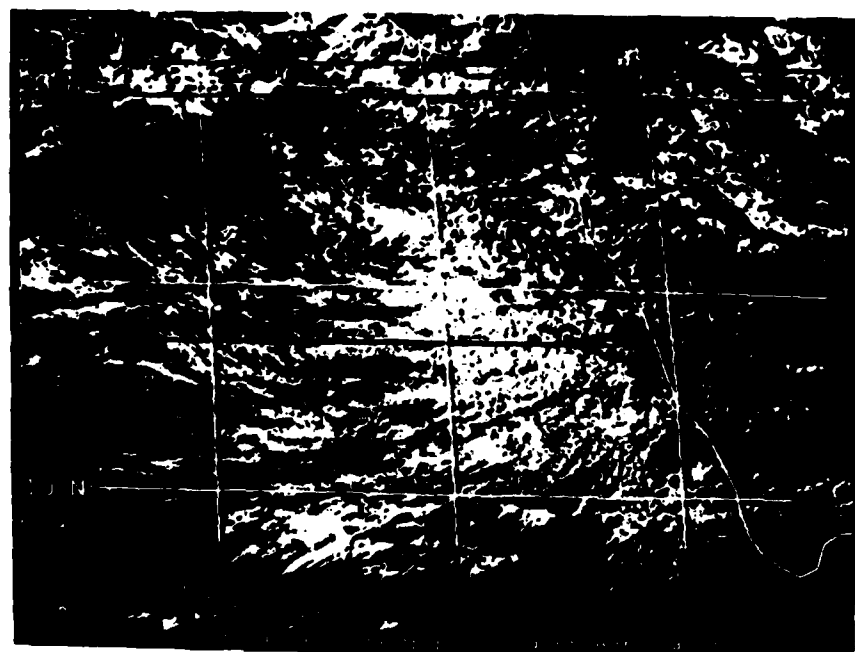
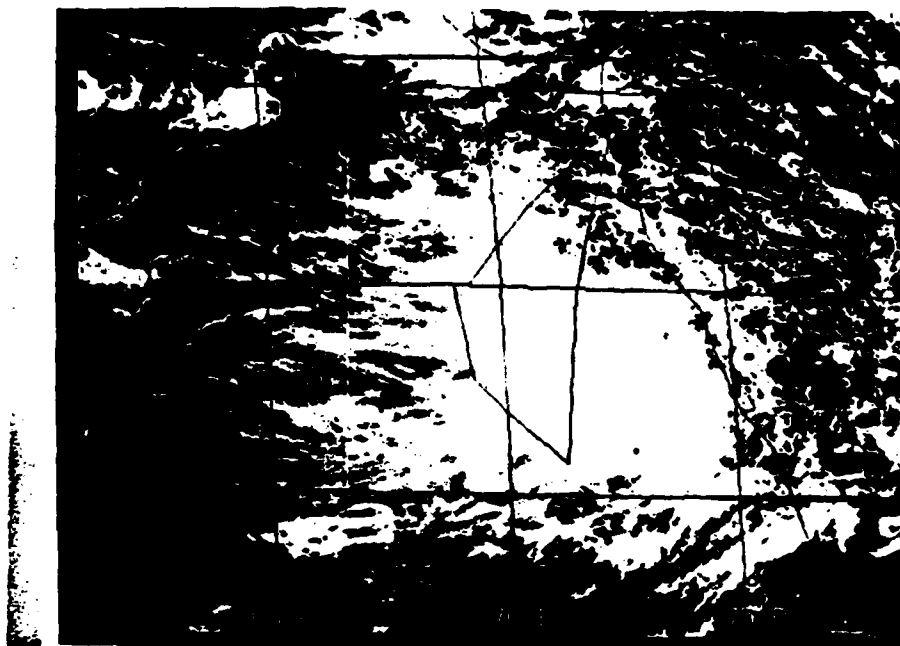


Fig. 6 GOES-I visual imagery for 20 June 1979: 0900 GMT (top), 1200 GMT (bottom).

suggested a series of convective bands that were oriented from $\sim 240^{\circ}$ - 060° (this orientation is roughly parallel to the low-level flow). Just west of the western edge of the cirrus shield, cumulus streets were noted feeding into the system from the west and west-southwest. Well defined cumulus streets are usually indicative of low-level flow exceeding 15 m s^{-1} .

By 1200 GMT on 20 June, bands of convection were clearly evident in visual satellite imagery (Fig. 6). A fascinating change in the cirrus canopy had evolved: distinct holes in the western flank of the cirrus shield were evident downwind (at the cirrus level) from the most intense convective bands. These more intense convective areas are evident in Fig. 6 as cumulonimbus tops protruding through the top of the cirrus shield. Concurrent infrared imagery at 1200 GMT revealed that these tops were the coldest in the entire convective cloud cluster. At least one band of cumulonimbi was long enough to be categorized as a squall line: this line of convection in infrared imagery (Fig. 7) was about 650 km long and was oriented along a 240° - 060° axis. The squall line was centered about 40 km north of station Amini (11.1°N , 72.7°E). The ultimate effect of this squall line upon the BL over Amini will be discussed in the next chapter. The 1200 GMT imagery also suggests that there was upper-level (cirrus level) diffluent flow. This is indicated because cirrus streamers are oriented towards the southwest in the lower left portion of Figs. 6 and 7, while the cirrus streamed to the northwest in

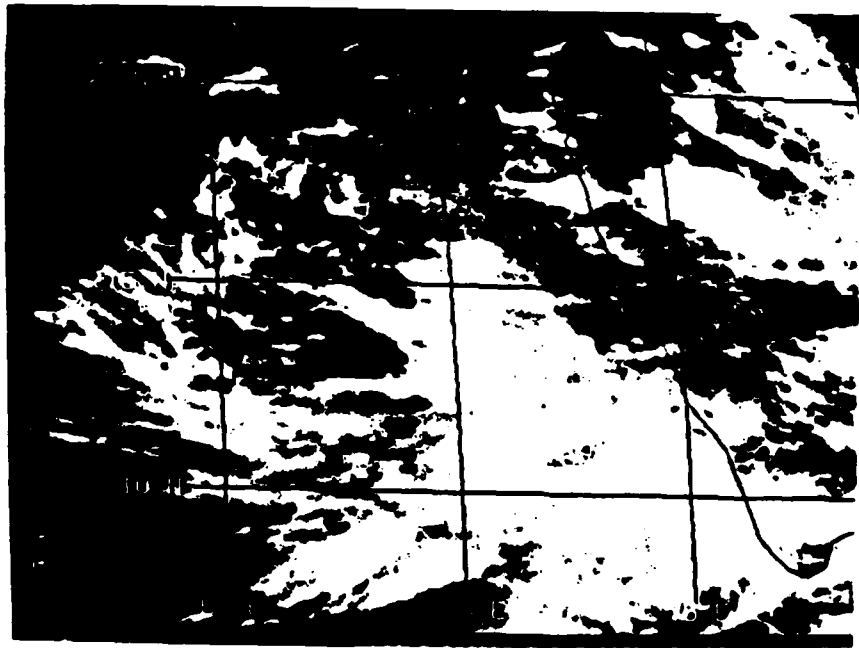
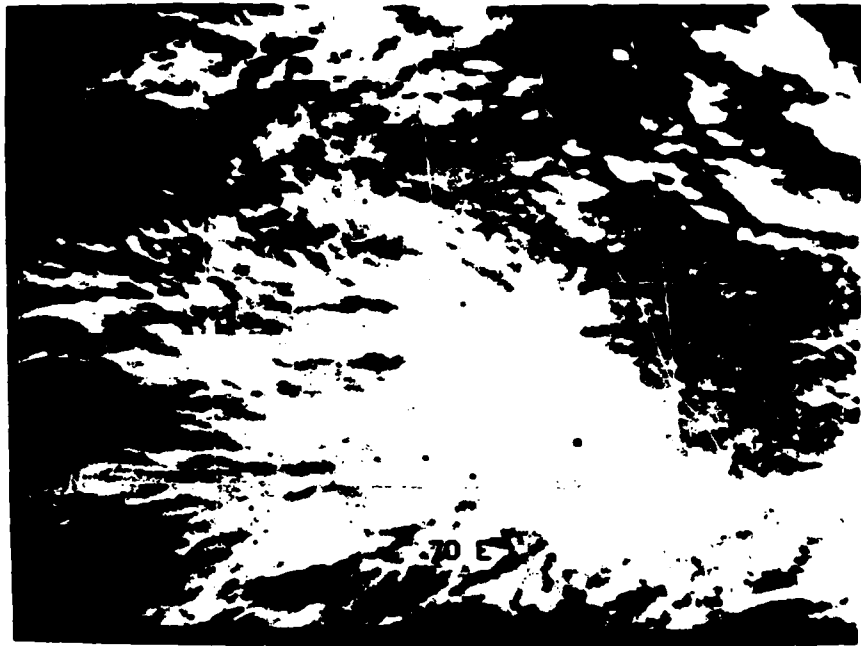


Fig. 7 GOES-I infrared imagery for 20 June 1979: 1200 GMT (top), 1500 GMT (bottom).

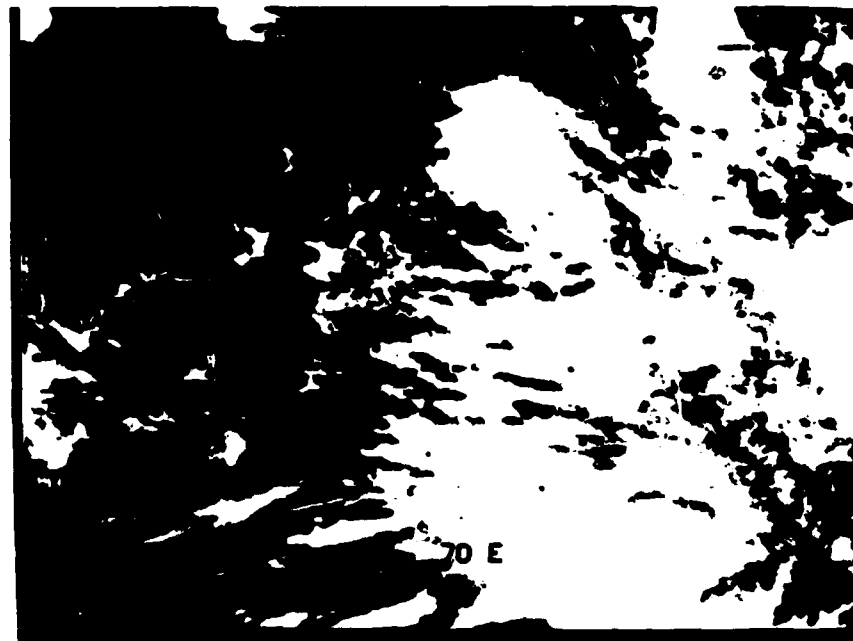
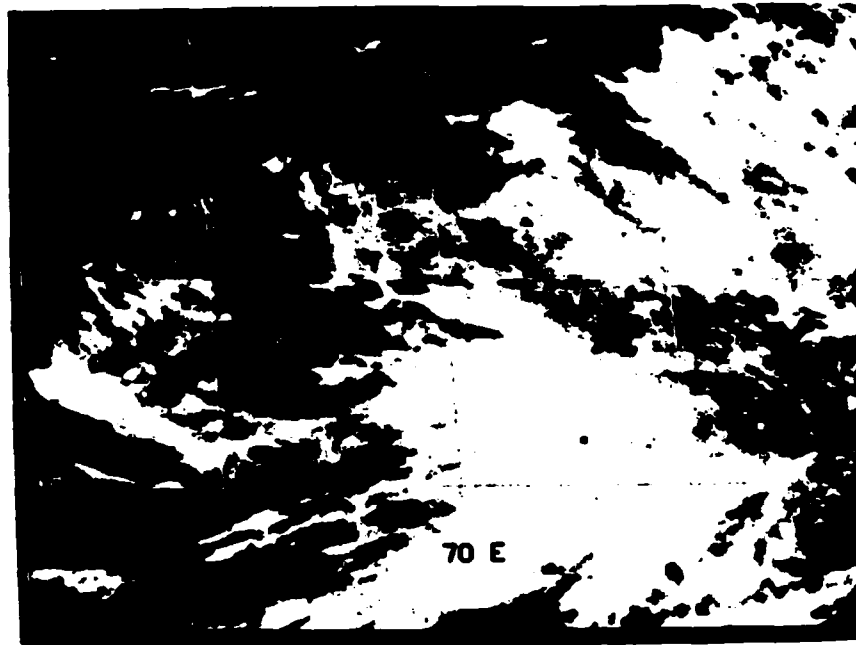


Fig. 8 GOES-I infrared imagery for 20 June 1979: 1800 GMT (top), 2300 GMT (bottom).

the upper left portion of the figures.

The 1500 and 1800 GMT infrared imagery (Figs. 7 and 8) depict the system becoming less concentrated as it apparently translated slowly to the southeast. By 2300 GMT on 20 June (Fig. 8), the once concentrated cloud cluster could really no longer be considered as a discrete weather system, as the convection merged with extensive convection over mainland India.

h. Kinematic fields

The following discussion will be centered around 1200 GMT on 20 June, since this was a standard rawinsonde data time. However some references will be made to 0600 GMT, since at about this time an abundance of aircraft winds were available from the Electra and AVRO aircraft. Kinematic fields are valuable for this study because as Ramage (1971) points out, pressure fields are of little value in relation to observable weather features during the southwest monsoon.

The surface flow on 20 June was typical for the early summer southwest monsoon over western India. The surface analysis for 1200 GMT (Fig. 9) depicts a deep low pressure trough over the central Arabian Sea. This trough caused the surface flow to be generally southwesterly over the east-central Arabian Sea, gradually becoming more westerly and decreasing in speed as India's west coast was reached. Ship and island reports indicated surface wind speeds over the open ocean were around $15-20 \text{ m s}^{-1}$.

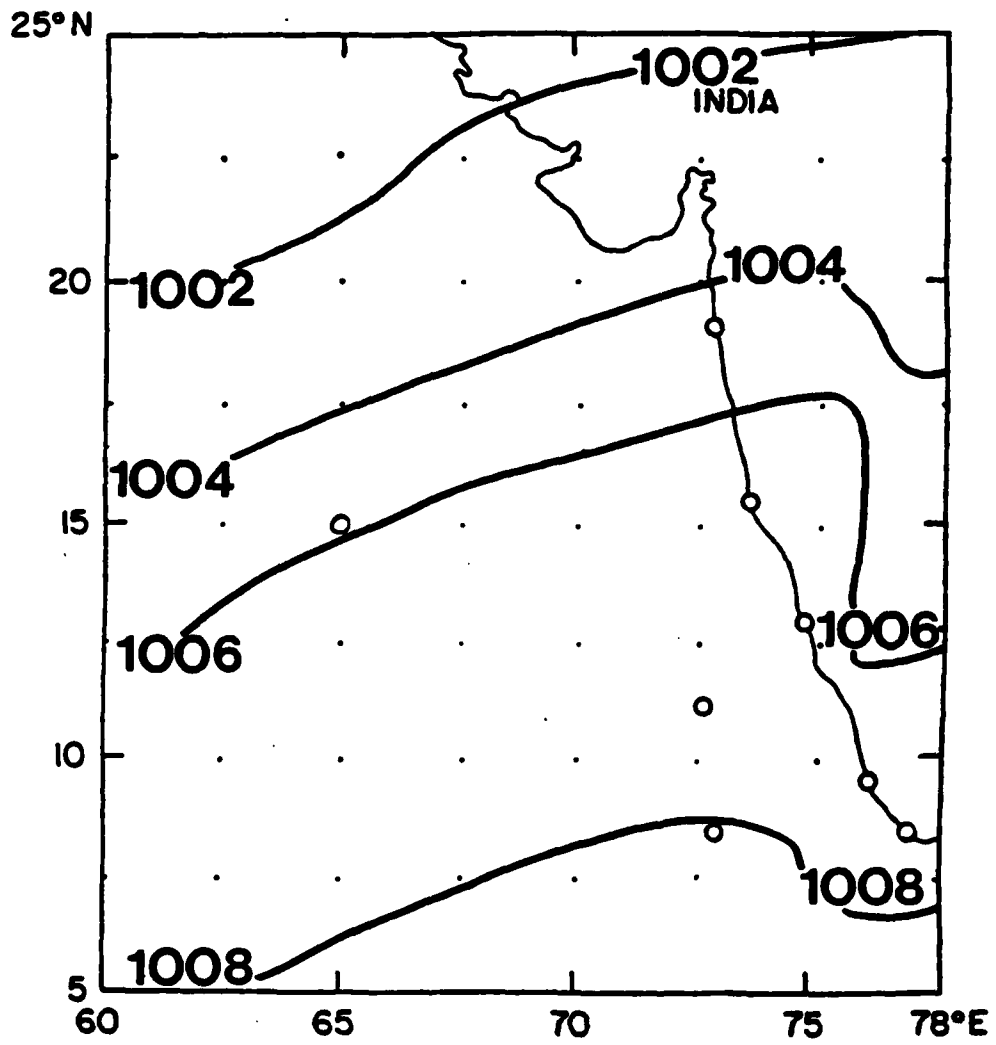


Fig. 9 Surface pressure analysis for 1200 GMT 20 June 1979.

However along India's west coast speeds were generally less than 5 m s^{-1} . This implies that the surface flow undergoes a marked deceleration from west to east across the central Arabian Sea to India's western coastline. This deceleration may be caused by the influence of India's western Ghat mountains (Grossman and Durran, 1982).

Flow above the surface in the BL remained generally westerly with height. Speeds throughout the entire troposphere at most stations peaked in the 900-850 mb layer (see Fig. 10). This is a direct influence of a branch of the Somalia jet (Pant, 1976). The highest spot wind measured by the Electra research aircraft was 25 m s^{-1} at 900 mb near 14.7°N , 69.2°E . This resembles wind profiles studied by Jambunathan *et al.* (1974) and Desai *et al.* (1976).

The obvious consequence of such a low-level wind pattern is that the convective cloud cluster is drawing low-level inflow from the west. Speeds of the flow decrease towards the coastline, making it highly convergent (especially around the 900 and 850 mb levels). When winds from research aircraft and DWS's are included, the wind field exhibits considerable mesoscale variability. A case in point is the 0600 GMT 900 mb winds (Fig. 11). The mesoscale variability of the low-level flow was also noted by scientists on board the Electra. It is logical to assume that mesoscale variations in the velocity fields will lead to mesoscale variations in computed divergence fields. Rao (1976) recog-

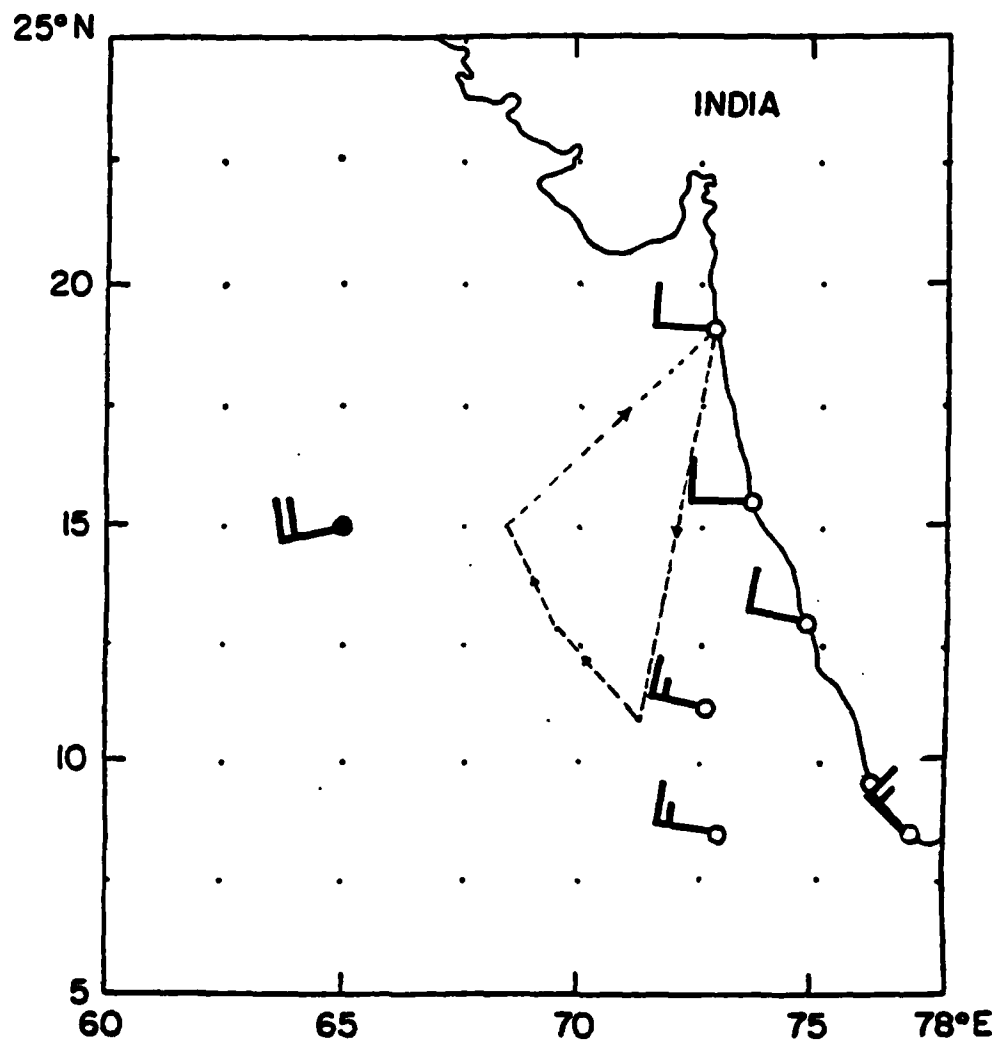


Fig. 10 900 mb winds ($m s^{-1}$) for 1200 GMT 20 June 1979. Open circles are actual observed rawinsonde winds. Full circles are interpolated (0600-1800 GMT) winds. Dashed line is flight track of the Electra.

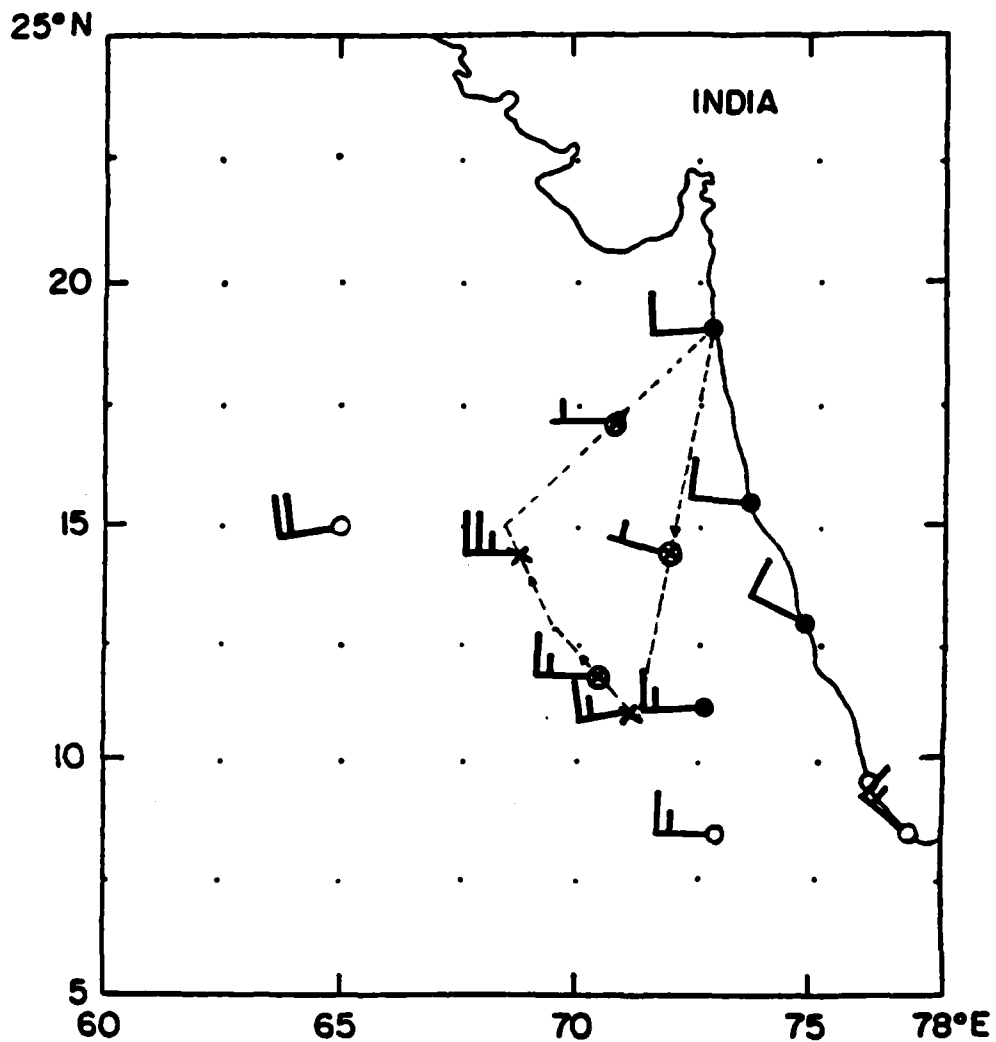


Fig. 11 900 mb winds (m s^{-1}) for 0600 GMT 20 June 1979. Open circles are actual observed rawinsonde winds, full circles are interpolated (0000-1200 GMT) winds. X's denote Electra spot wind measurements, \oplus 's denote DWS winds. Electra and DWS winds were used $\pm 1\frac{1}{2}$ h of 0600 GMT. Dashed line is flight track of the Electra.

nized that convergent fields were interacting on several scales over the eastern Arabian Sea. He concluded that this convergent interaction seems to strengthen organized bands of convection in this region.

Above 850 mb, the flow continued to be westerly but showed a monotonic decrease in speed with height up to 500 mb. A tropospheric speed minimum was found at about 500 mb (Fig. 12). Winds at this level were generally less than 10 m s^{-1} over the entire analysis area.

Above the 500 mb level, the flow became easterly and increased with height as the TEJ (~ 150 mb) became established over the southern tip of India. Although the 200 mb wind field is shown in Fig. 13, the upper tropospheric wind speeds continued to increase up to ~ 150 mb, where Minicoy (8.3°N , 73.0°E) reported winds of 060° at 37 m s^{-1} at 1200 GMT.

The tropospheric flow relative to the convective cloud cluster can be summarized as follows: a strong, nearly unidirectional westerly inflow occurs below 500 mb, but is strongest in the BL (~ 900 mb); above 500 mb the flow is also nearly unidirectional, but easterly, with speeds increasing with height to ~ 150 mb.

a. Divergence fields

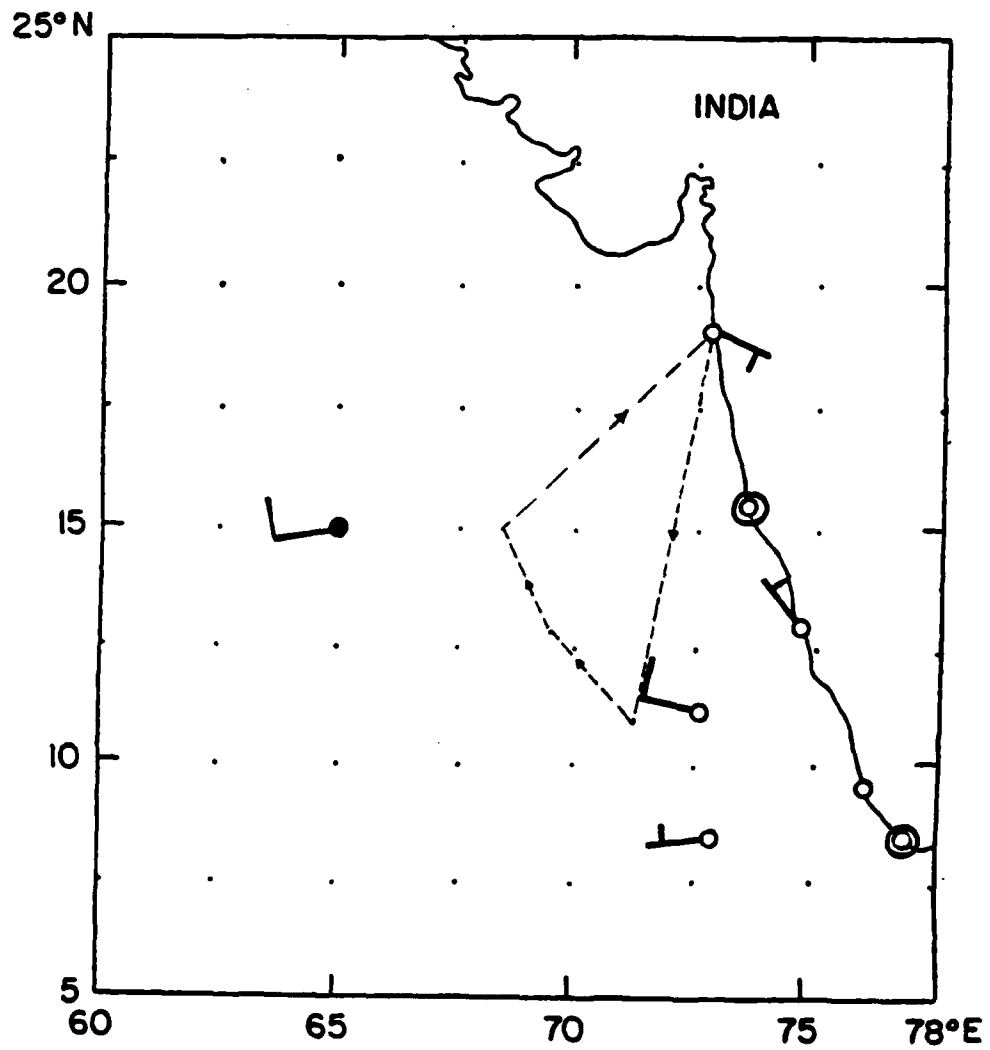


Fig. 12 500 mb winds ($m s^{-1}$) for 1200 GMT 20 June 1979. Open circles are actual observed rawinsonde winds. Full circles are interpolated (0600-1800 GMT) winds. Dashed line is flight path of the Electra.

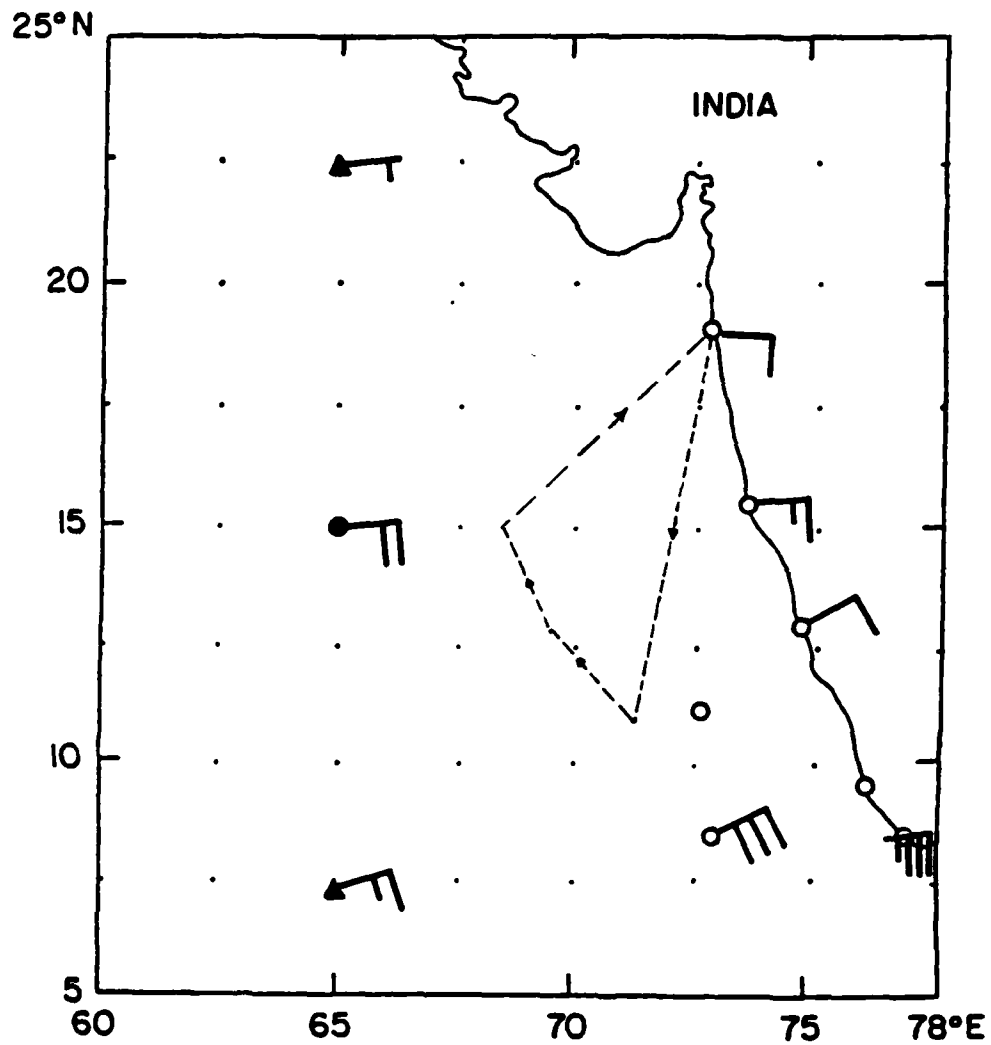


Fig. 13 200 mb winds (m s^{-1}) for 1200 GMT 20 June 1979. Open circles are actual observed rawinsonde winds. Full circles are interpolated (0600-1800 GMT) winds. Full triangles are satellite-derived winds. Dashed line is flight track of the Electra.

Divergence fields were computed over the analysis area using the equation:

$$D = \frac{\partial u}{\partial x} + \frac{\partial v}{\partial y} \quad (1)$$

where D is the horizontal velocity divergence and u,v are the zonal and meridional components of the wind velocity.

An 8 x 8 grid was centered over the analysis area (i.e., Fig. 1) with a grid spacing of 275 km. Rawinsonde winds were plotted on the grid, with data from the Quick Look 'Summer MONEX Atlas' Part II used to fill in data sparse areas. A subjective isogon/isotach analysis was then performed. Then u, v wind components were computed.

The finite difference expression to approximate Eq. 1 (Holton, 1979) was:

$$\frac{\partial u}{\partial x} + \frac{\partial v}{\partial y} = \frac{u(x_0+d) - u(x_0-d)}{2d} + \frac{v(y_0+d) - v(y_0-d)}{2d} \quad (2)$$

where d is the grid spacing, and x_0 and y_0 are the x,y coordinates for a reference grid point. Errors in divergence values using (2) could approach 20% near data sparse areas. Such errors could cause the sign of the divergence to be wrong where computed values are small. Thus, only the areas where divergence values are relatively far from zero are highlighted here.

The calculated 850 mb divergence field for 1200 GMT is shown in Fig. 14. The areas of maximum convergence (divergence values

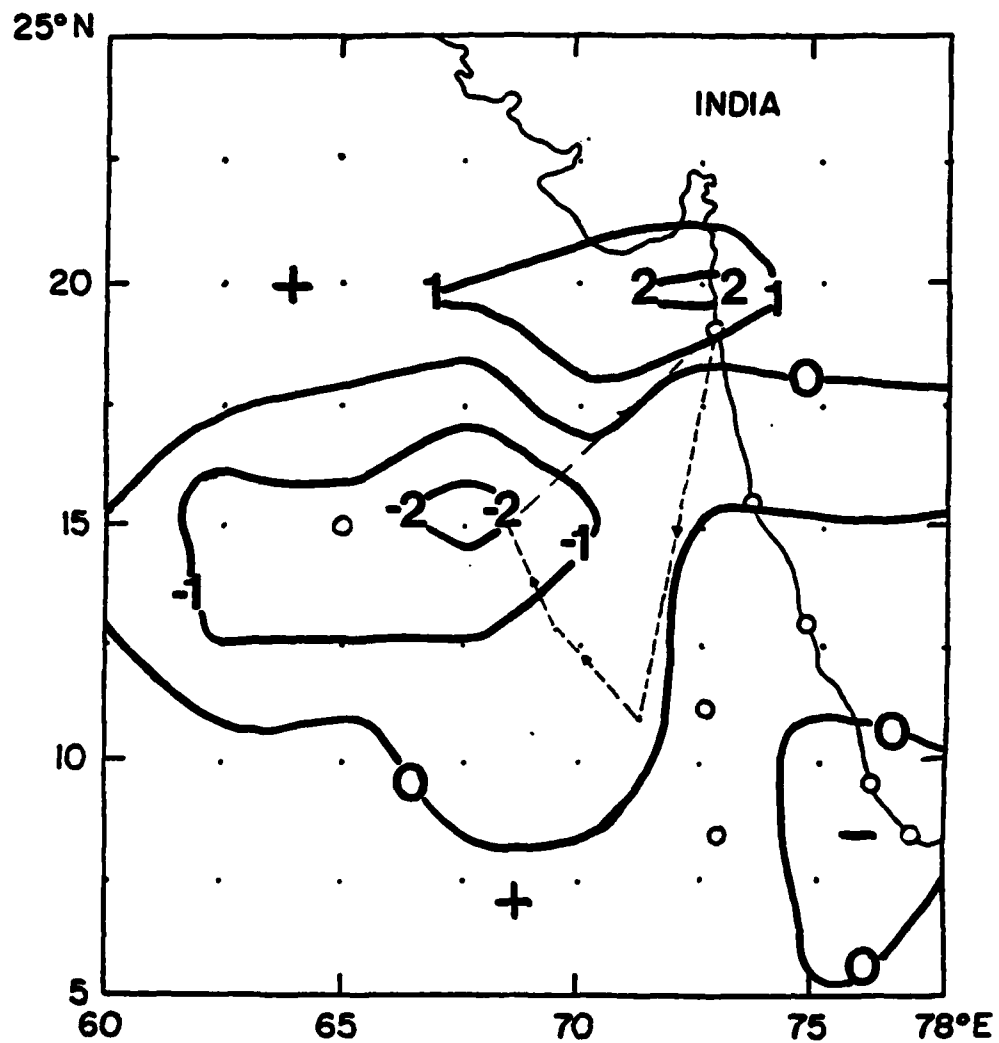


Fig. 14 Computed 850 mb divergence ($\times 10^{-5} \text{ s}^{-1}$) field for 1200 GMT 20 June 1979.

less than $-2.0 \times 10^{-5} \text{ s}^{-1}$) agree qualitatively well with the satellite observed areas of most intense convection (Fig. 6). Unfortunately, the wind data are not fine enough to resolve mesoscale variations in the 850 mb flow. Such measurements are obviously necessary if an attempt is made to relate mesoscale convergence/divergence patterns to the observed areas of convection.

Since the low-tropospheric flow remained westerly with height (with decreasing speeds), convergence decreased upward in the troposphere. Maximum convergence values at 700 mb were only about 55% of those computed at 850 mb.

The cirrus outflow from the convective cloud cluster was subjectively determined to be ~ 200 mb. Echo top measurements of sea convection of 11.0 km were made by the Bombay radar at 0605 GMT. At 0752 and 0810 GMT scientists aboard the AVRO aircraft estimated cumulonimbus tops to be near 35,000 ft (10.8 km). The divergence field for 200 mb at 1200 GMT (Fig. 15) shows strong divergence over most of the analysis area. The region of strongest divergence was diagnosed over the area containing the tallest cloud towers in the convective cloud cluster.

d. Thermodynamic considerations

All sounding data (rawinsonde and DWS) were processed to produce vertical profiles of specific humidity (q), virtual

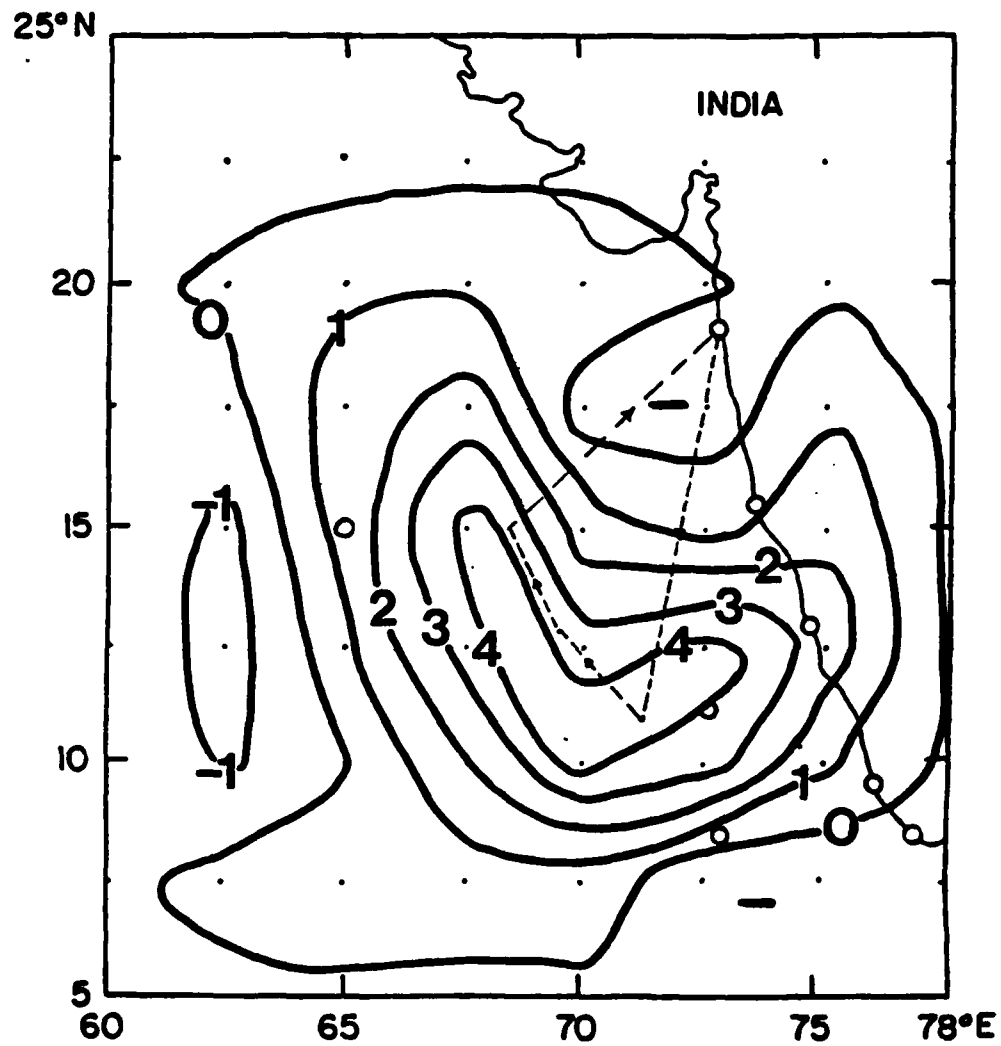


Fig. 15 Computed 200 mb divergence ($\times 10^{-5} \text{ s}^{-1}$) field for 1200 GMT 20 June 1979.

temperature (T_v) potential temperature (θ), virtual potential temperature (θ_v) equivalent temperature (T_e) and wet-bulb potential temperature (θ_w). Of these computed parameters, θ_v and θ_w were the most valuable for this study.

The moisture-related variables for DWS data are subject to the most error. For instance, the root mean square (RMS) error for DWS measured dew point depression was on the order of 1.25°C, while RMS error for temperature was on the order of 0.25°C (Bolhofer *et al.*, 1981). The moisture-related error is primarily a function of the humidity sensor's slow response time. Nevertheless, the DWS data is considered to be high quality (Krishnamurti *et al.*, 1979).

Profiles of θ_v are used in tropical studies because of their value in diagnosing mixed layer depths (Zipser, 1977). Vertical profiles of θ_v were computed using the equation (Fleagle and Businger, 1982):

$$\theta_v = \theta(1 + 0.61w) \quad (3)$$

where θ_v is virtual potential temperature, θ is potential temperature, and w is the mixing ratio. The top of the mixed layer was estimated to be at the inflection point of θ_v plots. This inflection point is where $\frac{\partial \theta_v}{\partial z}$ changed sign from negative to positive. Vertical profiles of θ_v are shown for research ship Deepak (15.0°N, 65°E) at 0600 GMT, and for the Electra's 0524 GMT DWS sounding (12.3°N, 71.3°E) in Fig. 16. Both profiles reveal a mixed layer depth of ~650 m. This value is typical for

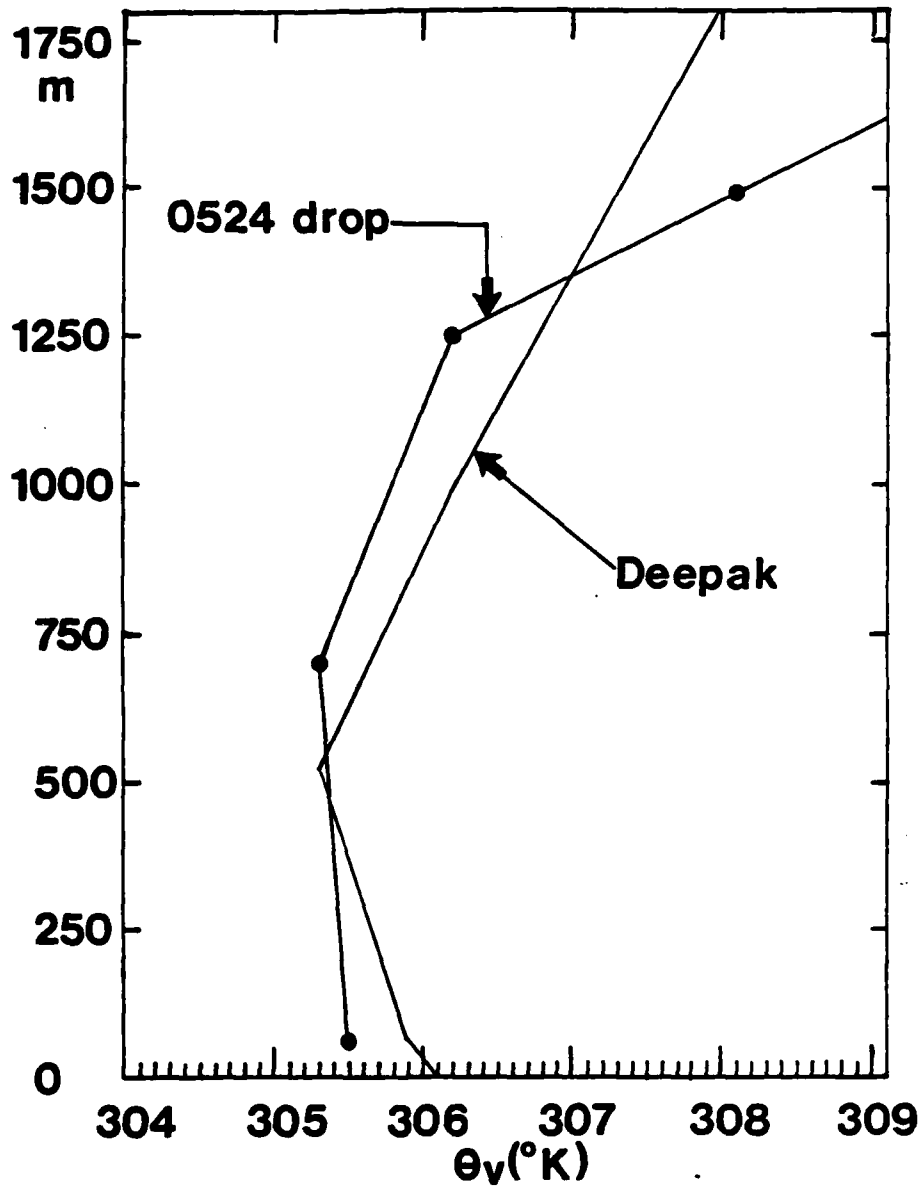


Fig. 16 Computed profiles of virtual potential temperature (θ_v) for ship Deepak (0600 GMT) and DWS #3 (0524 GMT) on 20 June 1979.

undisturbed (i.e., not modified by precipitating convection) flow over the eastern Arabian Sea. As will be discussed in Chapter 4, precipitating convection drastically alters oceanic mixed layer depths.

As an atmospheric tracer, θ_w is useful in the tropics because it is conserved under both moist and dry-adiabatic conditions (Wallace and Hobbs, 1977). Also, θ_w is also useful as a convenient label for air parcel energetics (i.e., high θ_w values can be referred to as "high energy air"). The use of θ_w in tropical squall line studies has been advocated by a number of authors (e.g., Houze, 1977; Mansfield, 1977; Zipser, 1977). Vertical profiles of θ_w in this study were computed by first generating the wet-bulb temperature at each pressure level by a computer program using an iterative technique. The wet-bulb temperatures were then plotted and θ_w 's were read directly off a thermodynamic diagram.

Vertical profiles of θ_w from the 0600 GMT ship Deepak sounding and the 0524 DWS sounding are displayed in Fig. 17. It is evident that the 0524 GMT profile is characterized by higher θ_w values at almost every level, although the slopes are similar. The 0524 GMT sounding, made near 12.3°N, 71.3°E, is 825 km east-southeast of Deepak. This implies the air gained energy as it progressed west to east across the eastern Arabian Sea. The reasons for this gain are the gradual increase of sea-surface temperatures of ~29°C near ship Deepak to ~30°C near the 0524 GMT

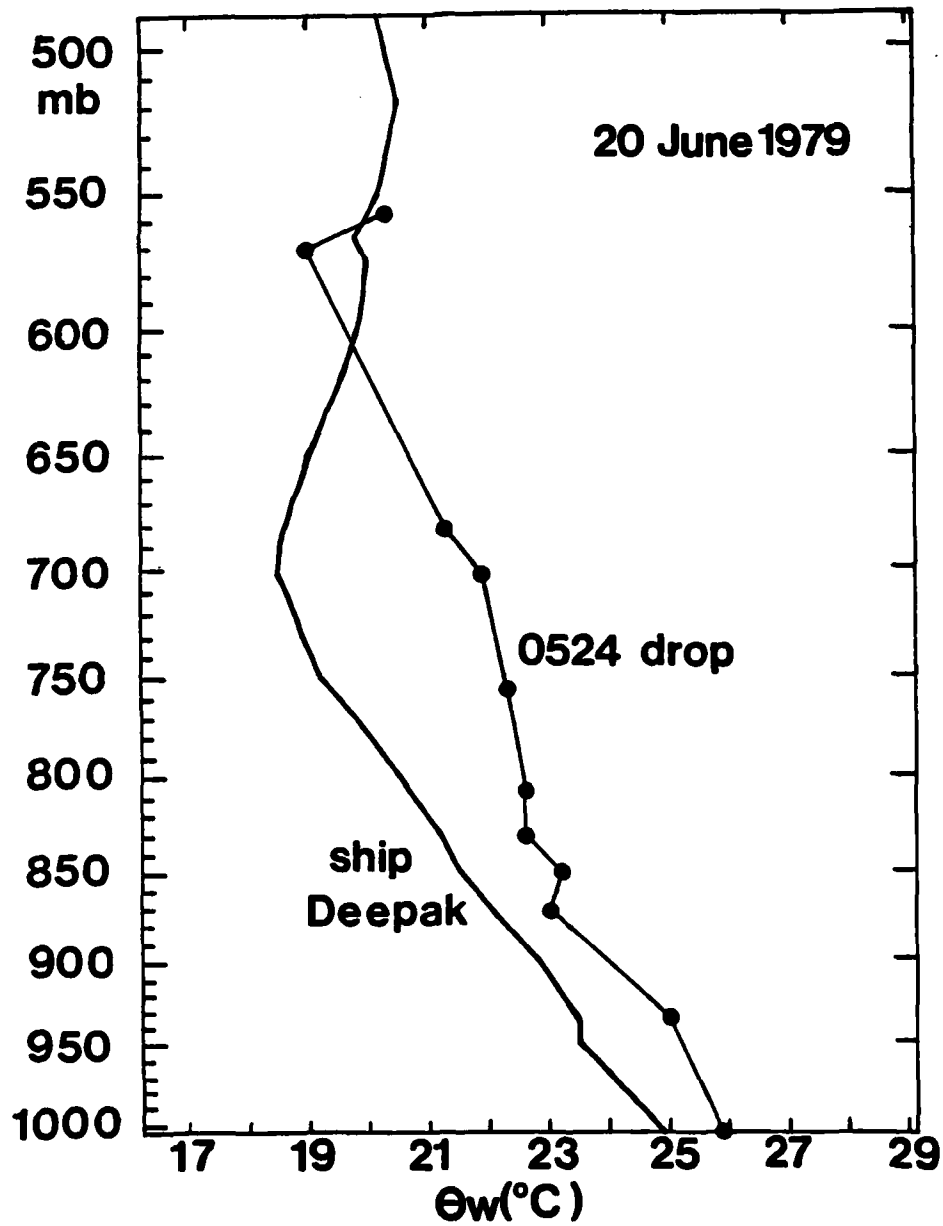


Fig. 17 Computed profiles of wet-bulb potential temperature (θ_w) for ship Deepak (0600 GMT) and DWS #3 (0524 GMT) on 20 June 1979.

sounding and the latent heat released by convection. The variation of the sea surface temperatures has long been recognized by a number of Indian monsoon researchers (i.e., Bhumralkar, 1978).

Convective instability can be defined (Haltiner and Williams, 1980) as $\frac{-\partial\theta_w}{\partial p} < 0$. In an absolute sense, the Deepak sounding was more convectively unstable through the lower to mid troposphere. From 1000 to 700 mb, the Deepak profile showed a $\frac{\partial\theta_w}{\partial p}$ of -2.1° per 100 mb, while 0524 GMT DWS profile revealed a value of -1.3° per 100 mb. However, the Deepak profile was drier than the 0524 GMT DWS sounding, and was in a region of no convective activity. The 0524 GMT DWS sounding, although less convectively unstable, was taken in the ambient air just ahead of a well-defined squall inside the synoptic scale convective cloud cluster. Hence the 0524 GMT profile is more characteristic of the unmodified air near the most active convection.

4. COMPONENT CONVECTION

a. Mesoscale blob profile

The Electra research aircraft departed Bombay at 0340 GMT on 20 June and made one DWS release at 0422 GMT before making a second DWS release at 0449 GMT (Fig. 2). Flying at 504 mb, the aircraft was in cloud and light rain. On board scientists noted that the drop was "...in area of convective activity." The cloud coverage and type at DWS release time was estimated to be 10/10 altostratus/nimbostratus. In fact the aircraft was entering the eastern side of an elliptically shaped convective mass within the convective cloud cluster. Such masses have been termed "mesoscale blobs" by LeMone and Zipser (1980). The term seems appropriate for the convective mass being discussed here. The UWSSEC's nephanalysis for 0600 GMT (along and inside the Electra flight track) is shown in Fig. 18. The convective mesoscale blob is clearly shown, extending across the aircraft's track. (Also note the linearly arranged convective area further south, which merged with the convective mesoscale blob later.)

The vertical profile of θ_w processed from the 0449 GMT DWS data is compared with the undisturbed (0524 GMT DWS) θ_w profile in Fig. 19. Despite the fact that the two profiles are only

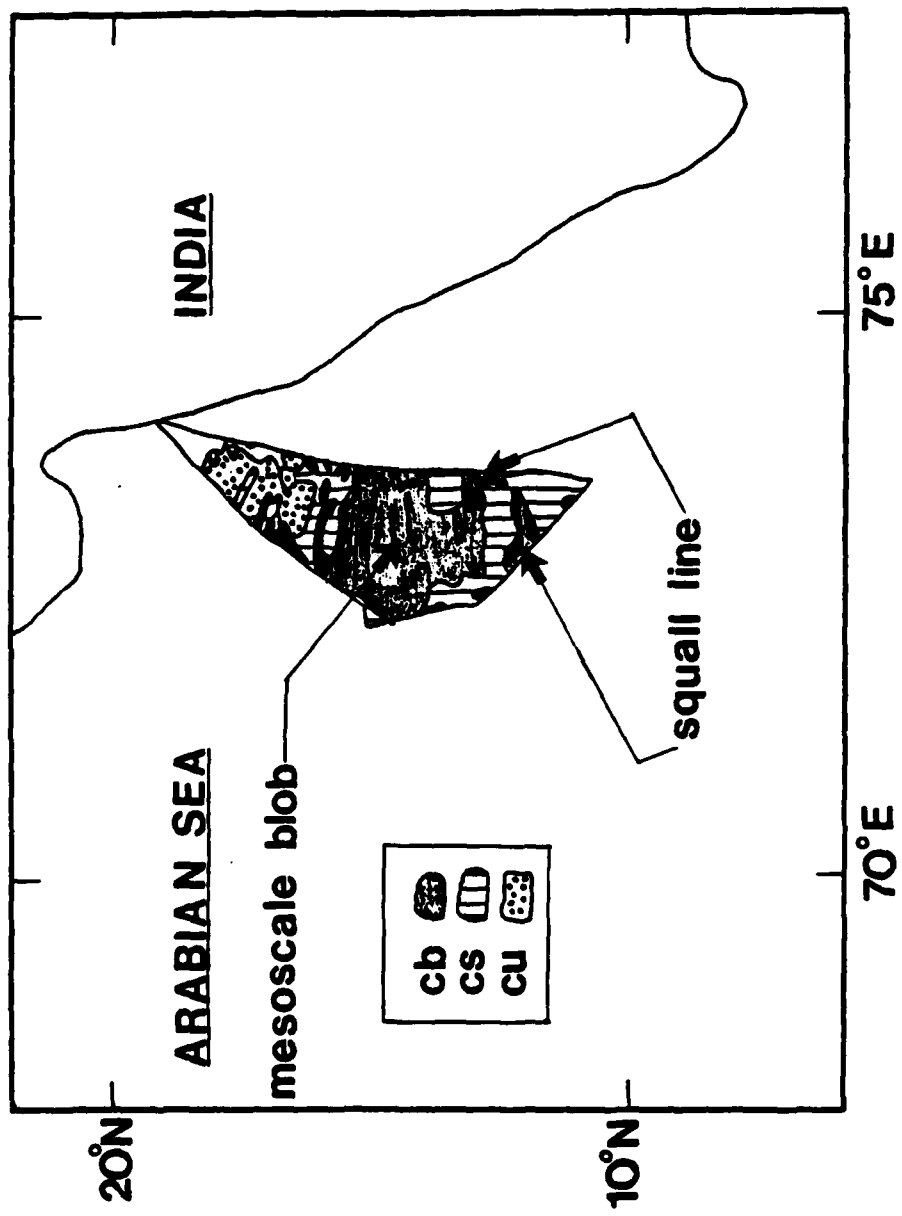


Fig. 18 UWSSEC's nephanalysis for 0600 GMT 20 June 1979.

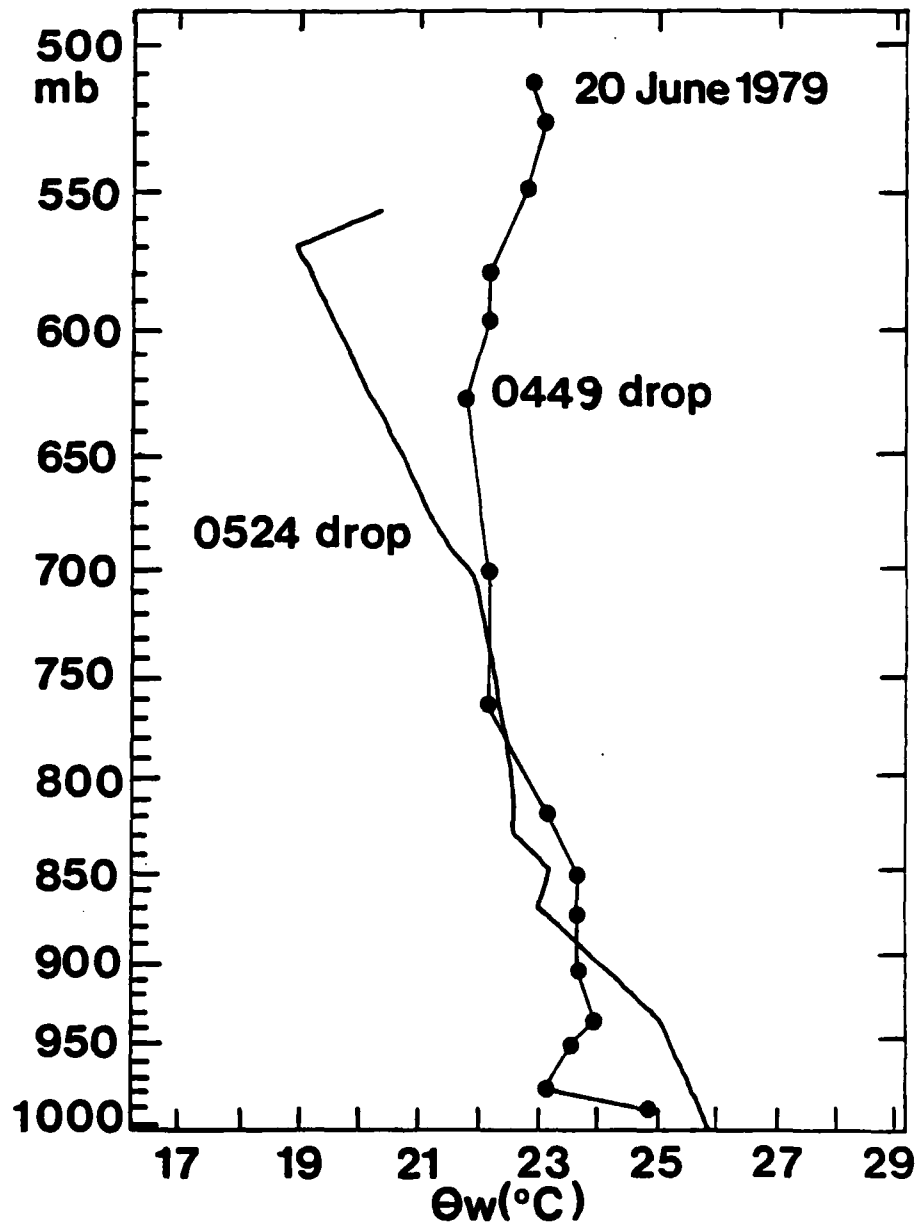


Fig. 19 Computed profiles of wet-bulb potential temperature (θ_w) for DWS #2 (0449 GMT) and DWS #3 (0524 GMT) on 20 June 1979.

separated by ~36 minutes in time and ~275 km in space, radically different profiles emerge. The greatest differences observed in the BL are at 980 mb, where a θ_w decrease of 2.5°C was observed. The substantial θ_w decreases below 885 mb were likely the result of an incursion of cooler convective-scale downdraft air into the BL (Zipser, 1977). Utilizing the value of θ_w as an atmospheric tracer, we attempt to find where the 1000 mb θ_w value of 24.9°C in the 0449 GMT profile could have originated from in the undisturbed atmosphere (0524 GMT profile). Apparently the near surface θ_w value of 24.9°C in the 0449 GMT sounding originated from around 927 mb (i.e., a short distance above the cloud base) in the undisturbed environment. There is no evidence that the lower energy BL air in the 0449 GMT profile originated from the mid-troposphere, e.g., vertical velocity measurements from the Electra's gust probe from 0447-0449 GMT at 504 mb revealed no negative values. The two profiles in Fig. 19 are quite similar from 892 mb to 740 mb. Above 740 mb, the 0449 GMT θ_w profile has much higher values. At 570 mb, the 0449 GMT θ_w value of 22.3°C is 3.3°C higher than the undisturbed 570 mb value of 19.0°C. It appears that high energy BL has been transported upward to the mid-troposphere. This thermodynamic overturning of the tropical atmosphere by active convection has been well documented (Riehl, 1979).

Mixed layer depths were inferred from the inflection point in θ_w profiles (Zipser, 1977). The undisturbed (0524 GMT) θ_w

profile yielded a mixed layer depth of ~650 m. As previously mentioned, this value is typical for the undisturbed summer eastern Arabian Sea atmosphere. The 0449 GMT θ_v (not shown) profile revealed a mixed layer depth of ~250 m. The cooling and shrinking of the tropical mixed layer by precipitating convection is responsible for such a low value for the mixed layer depth (Fitzjarrald and Garstang, 1981a).

b. Squall line profile

The UWSSEC 0600 GMT nephanalysis (Fig. 18) clearly showed a line of convection extending across the southern portion of the Electra's flight track. This squall line was encountered by the aircraft at about 0526 GMT, after launching the 0524 GMT DWS. A photo from the right side cloud camera (16 mm) taken at 0526 GMT (Fig. 20) clearly shows the line of cumulonimbus, with tops pushing through into the overcast just above the Electra's flight level. The left camera photo (taken also at 0526 GMT) shows the squall line's leading edge (Fig. 21). A well defined "shelf cloud" (arcus) extends downward and outward from the active cloud tower bases. Close examination of Fig. 21 reveals an arc of tiny scud below and ahead of the arcus cloud. This arc of small scud delineates where the leading edge of the cooler convective-scale downdraft air has progressed.

Soon after the 0526 GMT photos were taken, the Electra entered the squall line and began a 20 minute descent to begin a



Fig. 20 Electra cloud camera photo (right side) for 0526 GMT 20 June 1979. Flight level is ~510 mb.



Fig. 21 Electra cloud camera photo (left side) for 0526 GMT 20 June 1979.

series of BL measurements. The Electra was in cloud and precipitation (with some icing) for some 2.5 minutes after entering the squall line's leading edge. Since the airspeed of the Electra at this time averaged 140 m s^{-1} , this means the active band of cumulonimbus was about 20 km wide. A schematic diagram of the descent sounding is presented in Fig. 22.

The cloud structure changed dramatically from ahead (north) of the squall line to the rear (south). While the clouds in front of the squall line were predominantly cumuliform in nature, cloud camera photos (right side) taken at 0535 GMT show the area to be a "convective desert" (Fig. 23). The only low clouds were high based stratocumulus, and even these were quite thin. In this regard, the post-squall environment appears remarkably similar to the post-squall clouds described by Zipser (1977). The disparity between low cloud types ahead of and behind the squall line strongly suggests BL thermodynamic inhomogeneity.

During descent it was noted by on board scientists that the mid-level cloud above the Electra (which was an anvil cloud) was being sheared away from the active cloud towers along the squall line's leading edge. This was confirmed by satellite photos. The squall line was oriented along about a 240° - 060° axis which is parallel to the flow at the cloud base level. The 200 mb winds at 0600 GMT over the descent sounding area were 055° at 13 m s^{-1} . Assuming the 200 mb level is the cirrus outflow level, the anvil cloud is being sheared toward the southwest, or over the

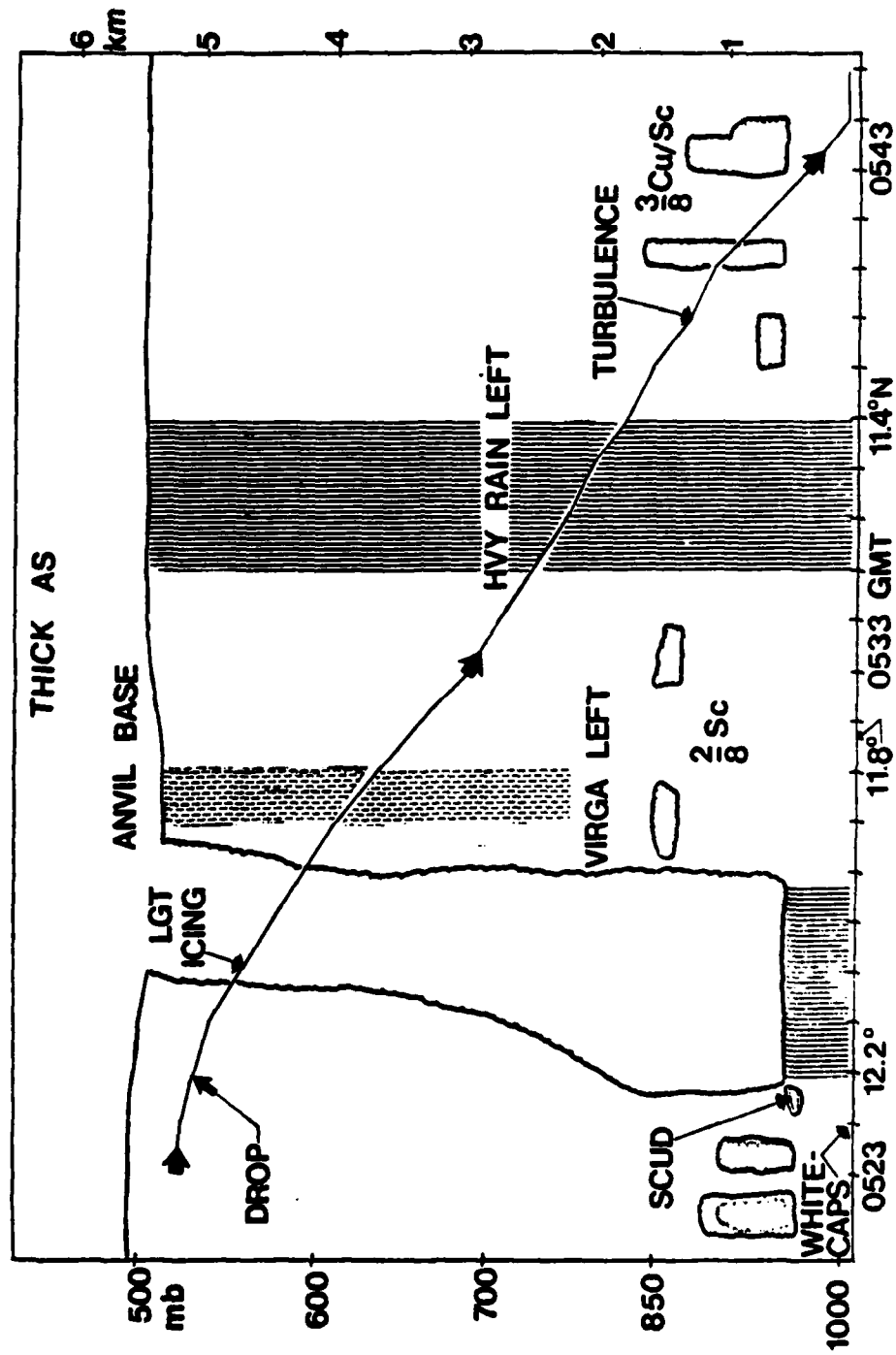


Fig. 22 Schematic of Electra descent sounding.

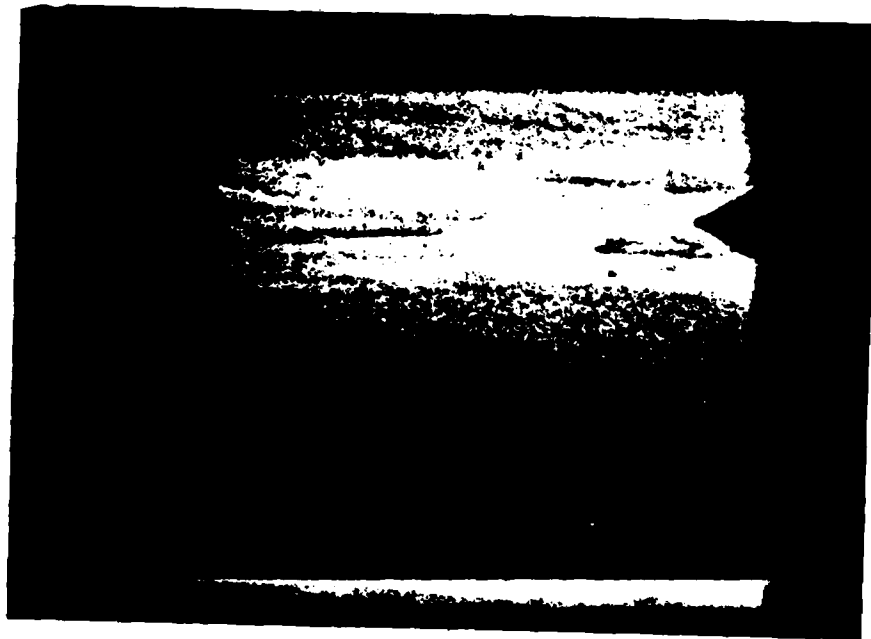


Fig. 23 Cloud camera photo (right side) for 0530 GMT 20 June 1979. Flight level is ~610 mb. Note the thick anvil above the aircraft, as well as the distinct absence of cumuliform cloudiness.

Electra as it made its descent sounding. The anvil cloud was not just cirrus debris, but was dynamically active (Houze, 1977). Virga was observed falling from the anvil on one occasion, and rain apparently was reaching the surface (see Fig. 22). Based on descent data, it appears that the anvil was ~7.0 km thick. Zipser (1977) states that he has personally observed many anvils in the 6-10 km thick range. Radiatively, such a thick anvil must be of considerable consequence. Data from the Electra's Eppley radiometer (recorded at 1 s^{-1}) indicated downward shortwave irradiance values of $\sim 120 \text{ w m}^{-2}$ while the aircraft was performing its descent sounding. Nearly clear sky irradiance values of 800-900 w m^{-2} were measured shortly after the Electra departed Bombay.

Computed profiles of θ_w for the undisturbed pre-squall environment (0524 GMT DWS) and the post-squall environment are shown in Fig. 24. It is readily seen that the descent sounding was characterized by lower energy air up to about 645 mb. Maximum θ_w decreases in the BL were at about 940 mb where a decrease of 1.8°C was noted. The 1000 mb θ_w value from the descent sounding suggests that this air descended from 955 mb in the pre-squall air, i.e., from near the cloud base (similar to the mesoscale blob case). Miller and Betts (1977) stated that in their study of convective squall lines over Venezuela that:

There is considerable evidence that there is indeed a downdraft originating from the layer above the cloud base in front of the storm. (p. 836)

Moncrief and Miller (1976) reached similar conclusions in their

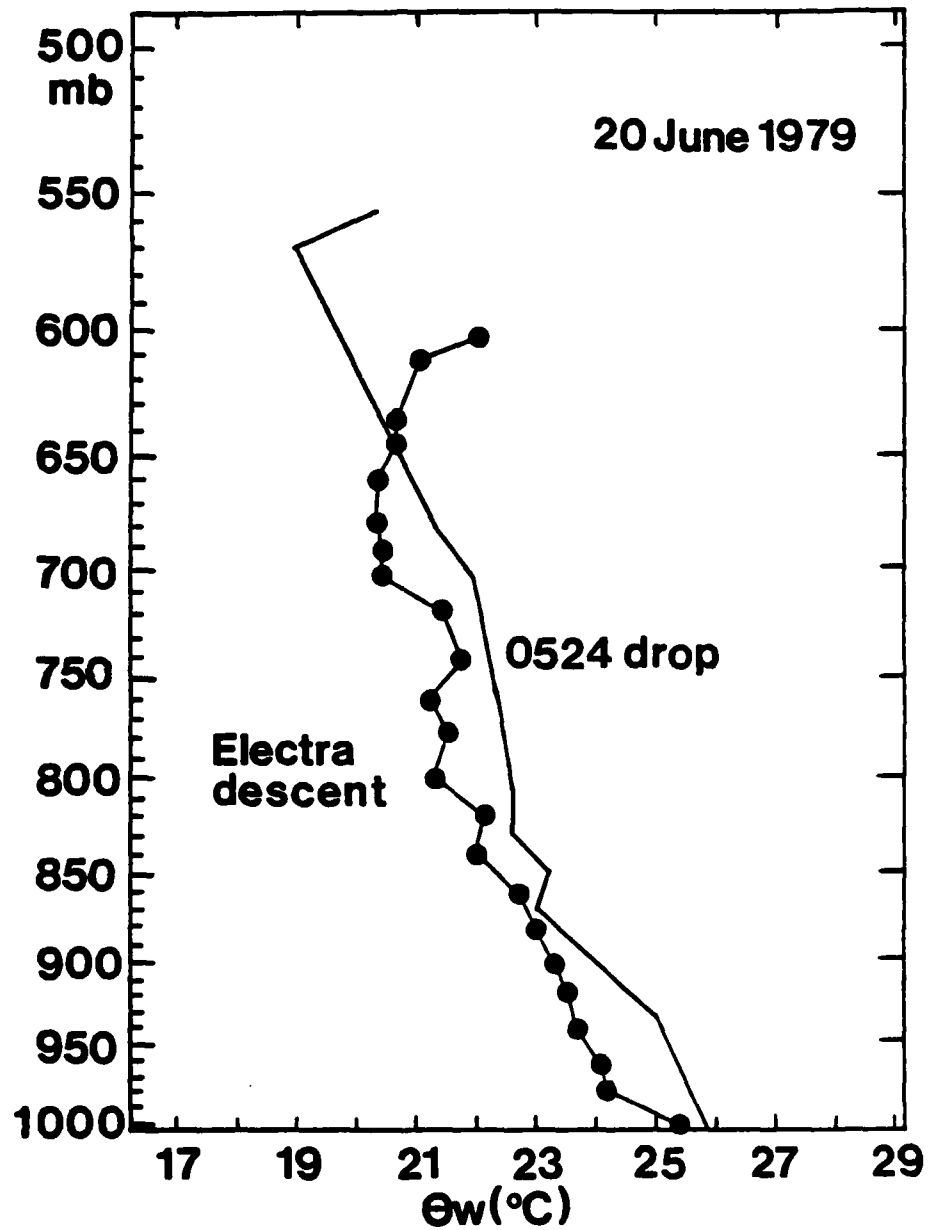


Fig. 24 Computed profiles of wet-bulb potential temperature (θ_w) for DWS #3 (0524 GMT) and descent sounding for 20 June 1979.

numerical simulation of Venezuelan squall lines.

The descent θ_v profile (not shown) yielded a mixed layer depth of ~200 m, a 55% decrease from the pre-squall sounding. Since the BL measurements were taken some distance (~90 km) south-southwest of the leading edge of the squall line, it is likely the BL was already recovering from the effects of the convective-scale downdrafts from the squall line to the north. This region fits the description of a "wake" region behind a squall line (Fitzjarrald and Garstang, 1981b; Johnson and Nicholls, 1983). The BL θ_v profile from the descent sounding is in excellent agreement with Zipser's (1977) for the region 100-150 km behind the squall's leading edge (Fig. 25). Indeed, Meyer (1982), reached the same conclusion for this general area using turbulent flux calculations. He concluded that this general area was in the wake region behind a squall line.

Examination of the T, T_d curves (Fig. 26) of the descent sounding show a pronounced subsidence inversion from 720-700 mb, with the T, T_d curves again meeting each other at 600 mb. Warner (1982) concluded that this sounding was characterized by "...a history of subsidence." He did not elaborate. The sounding in Fig. 25 strongly resembles the "diamond shape" of post-squall soundings described by Zipser (1977). The descent sounding is much drier and warmer than 0524 GMT DWS data above about 975 mb. Maximum warming was near 870 mb, where a temperature increase of 2.1°C was observed. Maximum drying occurred near 810 mb, where a

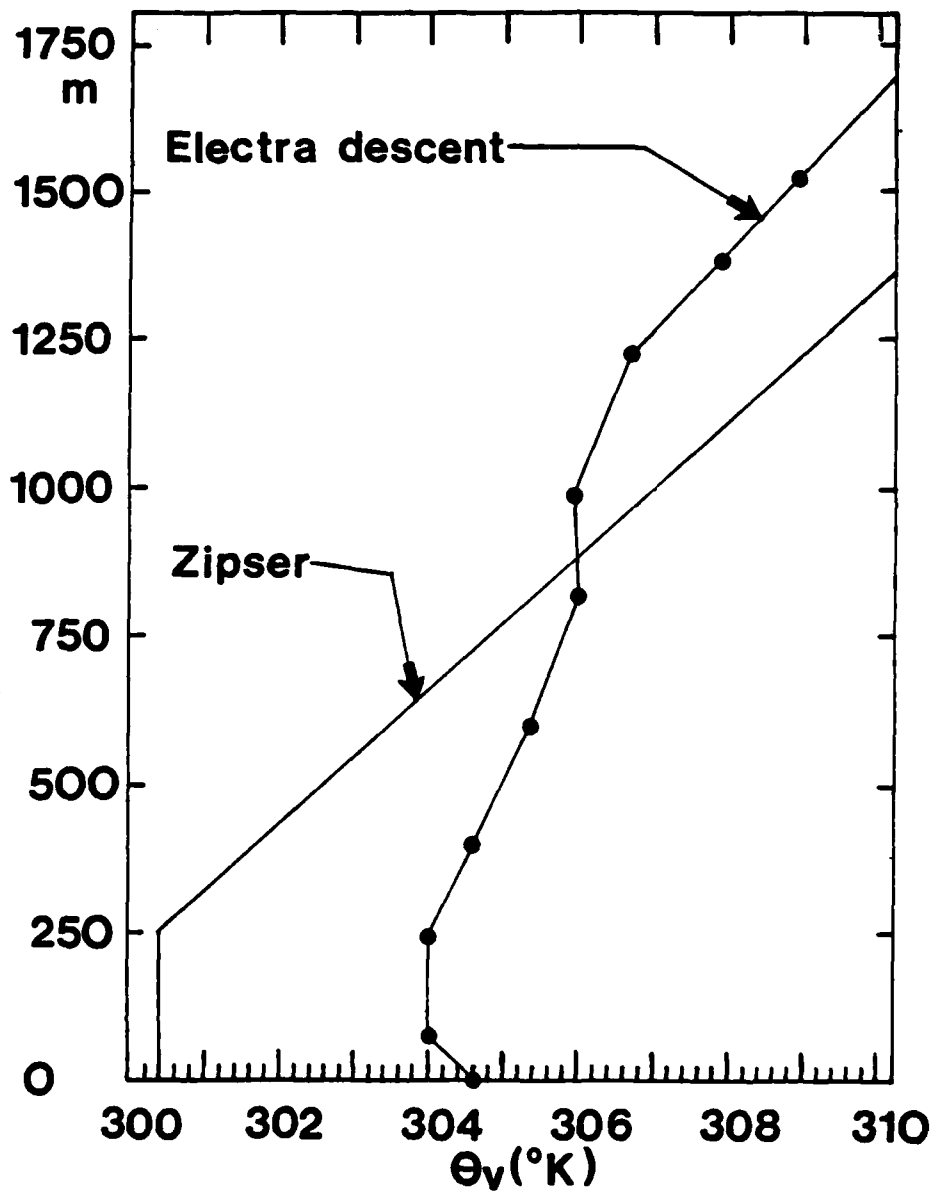


Fig. 25 Computed profile of virtual potential temperature (θ_v) for descent sounding and Zipser's idealized (1977) θ_v profile for 100-150 km behind a squall line.

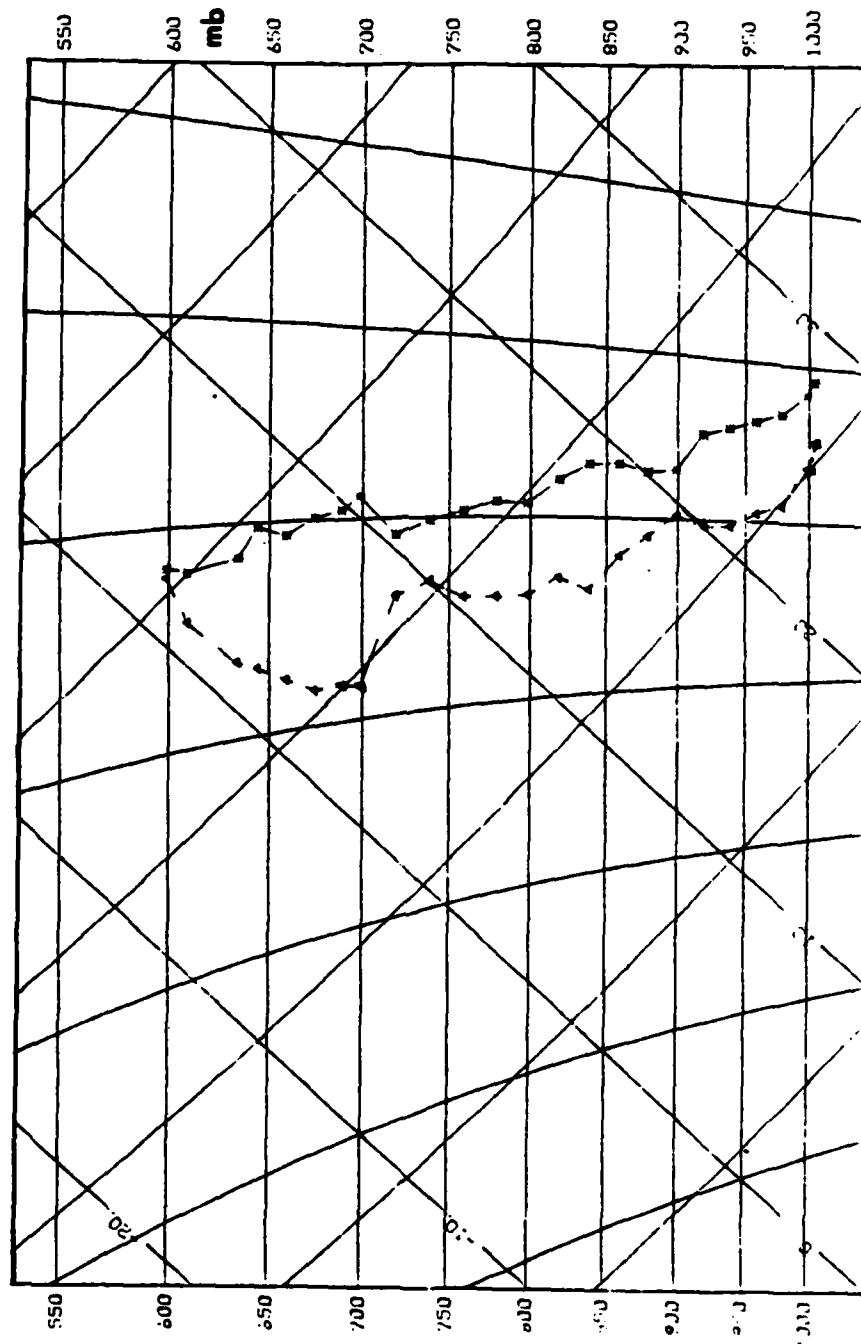


Fig. 26 Temperature (solid) and dew point (dashed) traces for descent sounding.

decrease in q of 3.5g/kg was noted. The warming and drying of the atmosphere behind a tropical squall line is well documented (Hamilton and Archbold, 1945; Johnson and Nicholls, 1983). This warming and drying is caused by mesoscale subsidence beneath the anvil cloud, as air descends in unsaturated downdrafts from the mid to lower troposphere (Zipser, 1969 and 1977). Examination of the extremely low θ_w values in the descent profile at 700 mb (Fig. 24) strongly suggests descent from ~630 mb. The aircraft observations of virga and rain falling from under the anvil cloud into the air below certainly suggest evaporation and concurrent cooling could be taking place. This is undoubtedly what initiated the mesoscale descent in the descent sounding area.

In the descent sounding area, both convective-scale and mesoscale downdrafts appear operative. This resulted in a very stable thermal stratification. Meyer (1982) found this region so stable that downward momentum fluxes in the lower BL were inhibited. This effectively de-coupled lower BL air from the high speed winds from around 900-850 mb. As Grossmann and Durran (1984) have pointed out, the anvil cloud in Arabian Sea convection tends to be sheared by the upper-level easterlies back over the high energy inflow air from the west. This is very different from GATE convection, where the high energy inflow air in the BL was unaffected by mesoscale subsidence from the anvil. This was because the anvil tended to be sheared away from the inflow air. After completing the descent sounding, the Electra made low-level

turbulence measurements near 11°N , 71.5°E (see Fig. 3). Details of these measurements were discussed by Meyer (1982).

By 0630 GMT the aircraft progressed northwestward at 950 mb. The aircraft passed through a detached thunderstorm at 0640 GMT. Upward looking measurements of shortwave irradiance values dropped from $\sim 70 \text{ W m}^{-2}$ (under the thinning anvil from the squall line) to $\sim 20 \text{ W m}^{-2}$ by 0641 GMT (Fig. 27). Scientists' notes at 0641 included "...beneath dark rain clouds with some lightning..." and "CBS to the right along a line." The aircraft continued northwestward where the weather improved briefly before the Electra entered the southwestern portion of the previously described squall line. The shortwave irradiance values decreased from $\sim 50 \text{ W m}^{-2}$ at 0644 GMT to 0 W m^{-2} just after 0645 GMT. The aircraft's weather radar was operating at a 35 km range at this time. Sketches of radar echoes from on board scientists clearly show a line of precipitating cumulonimbus and cumulus congestus extending across the flight track in a 240° - 060° orientation. Estimated surface winds (from observed sea states) increased markedly from 12.5 to about 17.5 m s^{-1} as the aircraft moved to the northern edge of the squall line. After the squall line was exited (0655 GMT) a second series of BL measurements were made. Meyer (1982) concluded that this area was quite unstable.

After the turbulence measurements were completed, the Electra made an ascent sounding from 0822-0842 GMT as the aircraft ascended from a pressure level of $\sim 1000 \text{ mb}$ to $\sim 482 \text{ mb}$. A

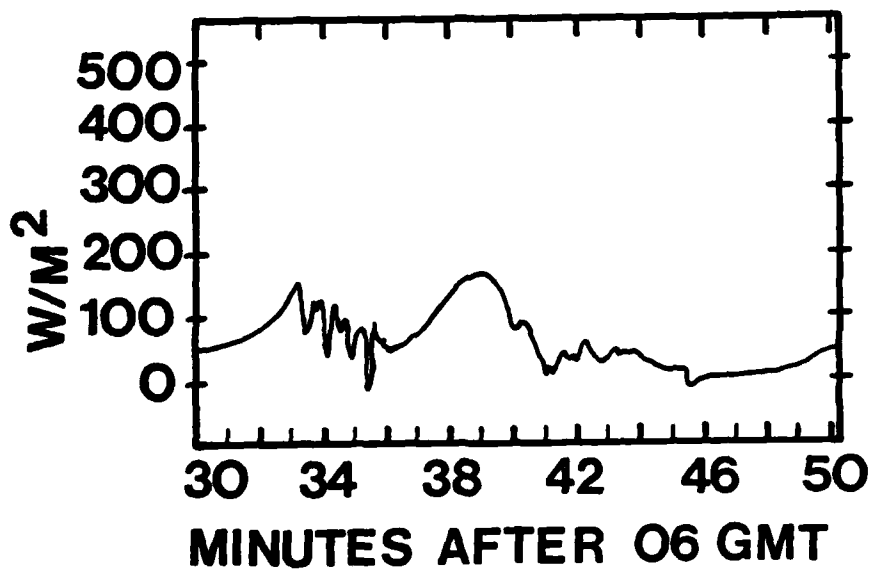


Fig. 27 Electra upward looking Epply radiometer shortwave irradiance trace.

schematic of the ascent sounding is presented in Fig. 28. The ascent sounding θ_w profile is compared with the 0524 GMT DWS sounding (pre-squall) in Fig. 29. Examination of the figure reveals very little difference below 675 mb. θ_w values are higher above this level in the ascent profile probably because ascent measurements were made in developing cumulus congestus. Warner (1983), using data from the ascent sounding, concluded that the data "...corresponds with the presence of cumulus." He made no further elaboration.

c. Thunderstorm profile

The Electra made its last DWS sounding on 20 June at 0901 GMT near 16.9°N, 70.6°E. This position was along the northeastern edge of a small thunderstorm cluster ~75 km wide (somewhat north of the larger convective mesoscale blob described earlier). The 0900 GMT GOES-I satellite imagery is shown in Fig. 6. The thunderstorm cluster is clearly evident, with the anvil being blown west-northwest by the upper-level easterlies (200 mb winds in this area at 0900 GMT were from 090° at 10 m s⁻¹). The θ_w profiles for the ascent sounding and the 0901 GMT DWS sounding are displayed in Fig. 30. Despite the fact that the two profiles were only separated by ~275 km in space and ~30 minutes in time, different profiles emerged, especially in the BL. The most obvious difference in the BL is the incursion of low θ_w air below 915 mb. The 1000 mb θ_w value of 24.0 in the 0901 GMT profile is the

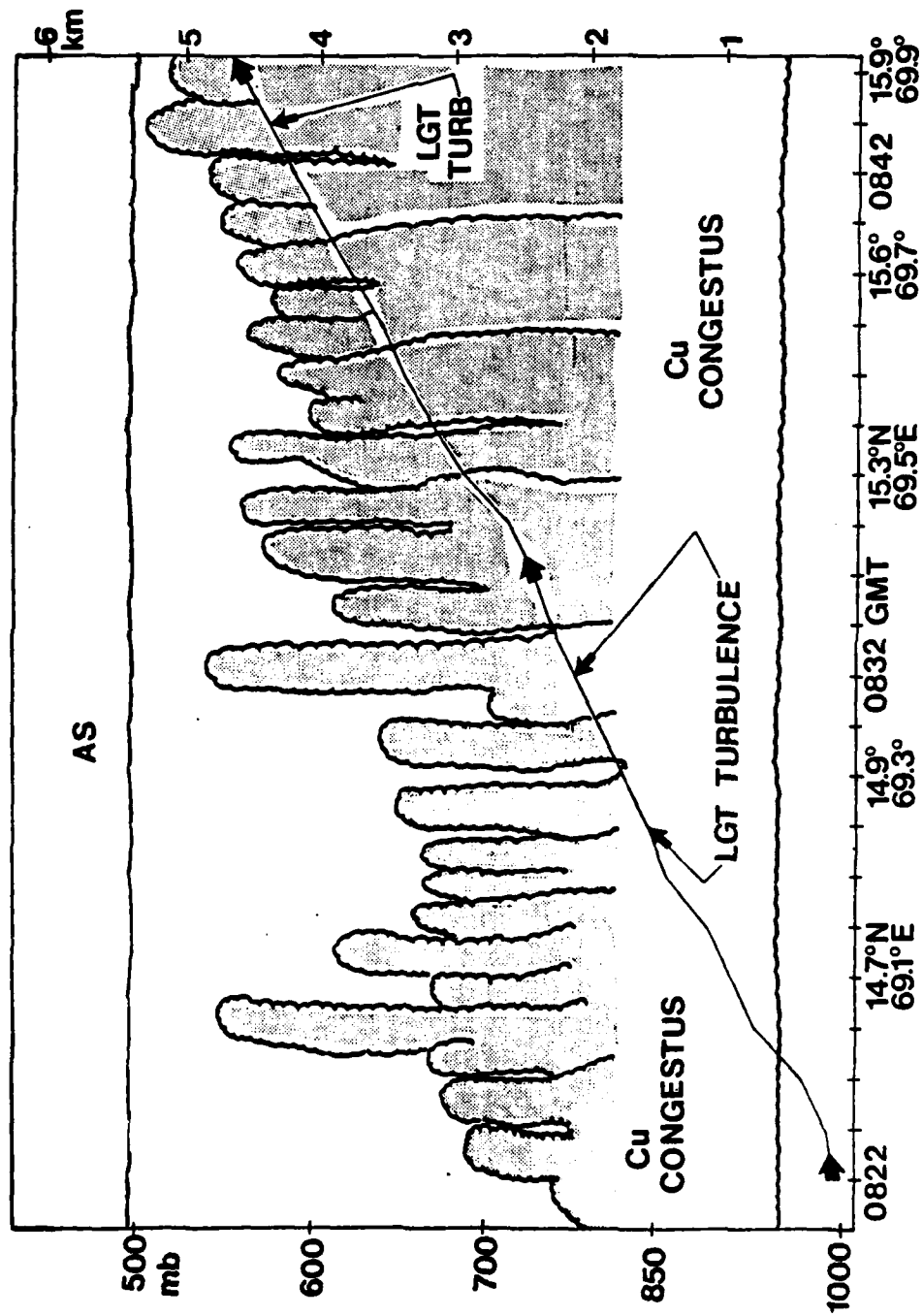


Fig. 26 Schematic of Electra ascent sounding.

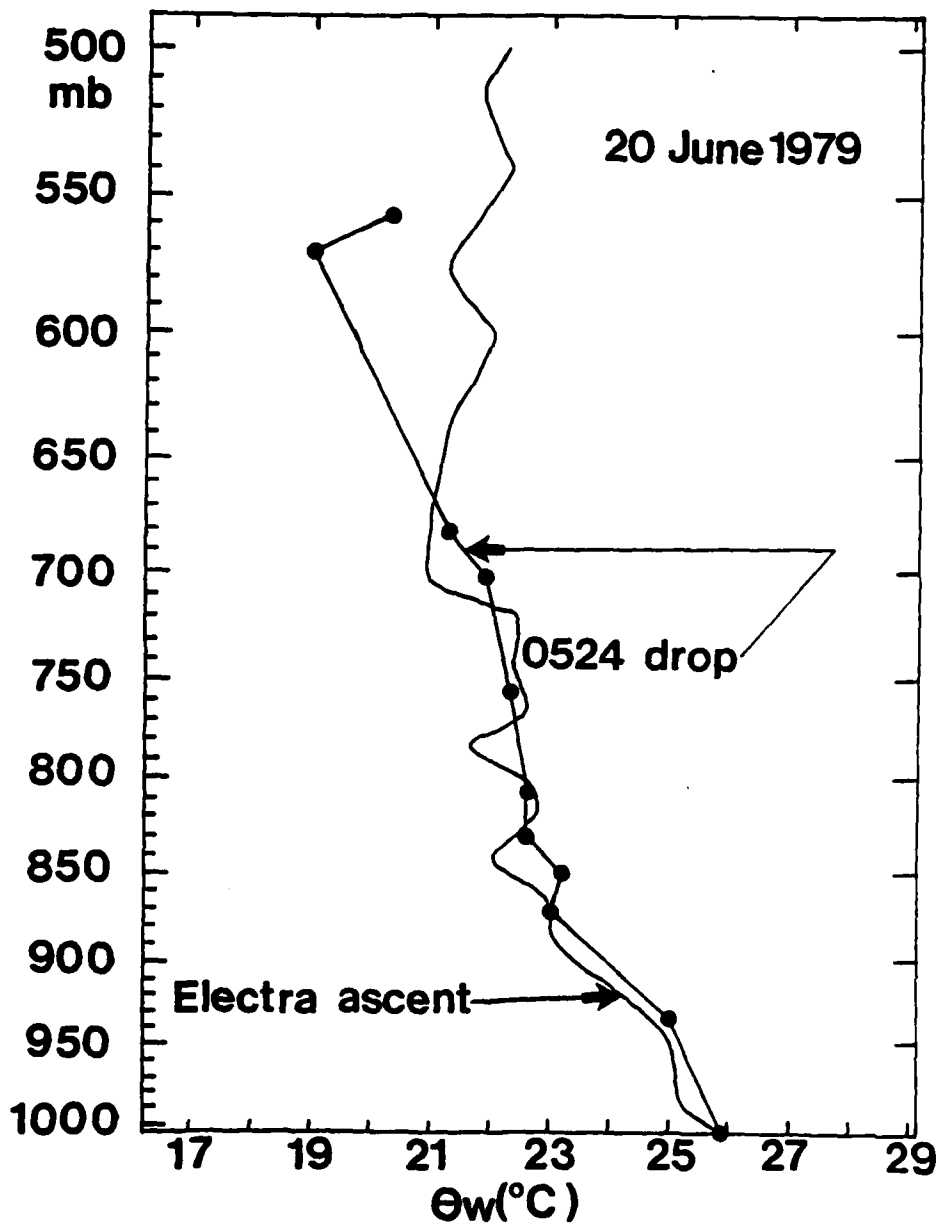


Fig. 29 Computed profiles of wet-bulb potential temperature (θ_w) for DWS #3 (0524 GMT) and ascent sounding. Note the similarity of the profiles in the BL.

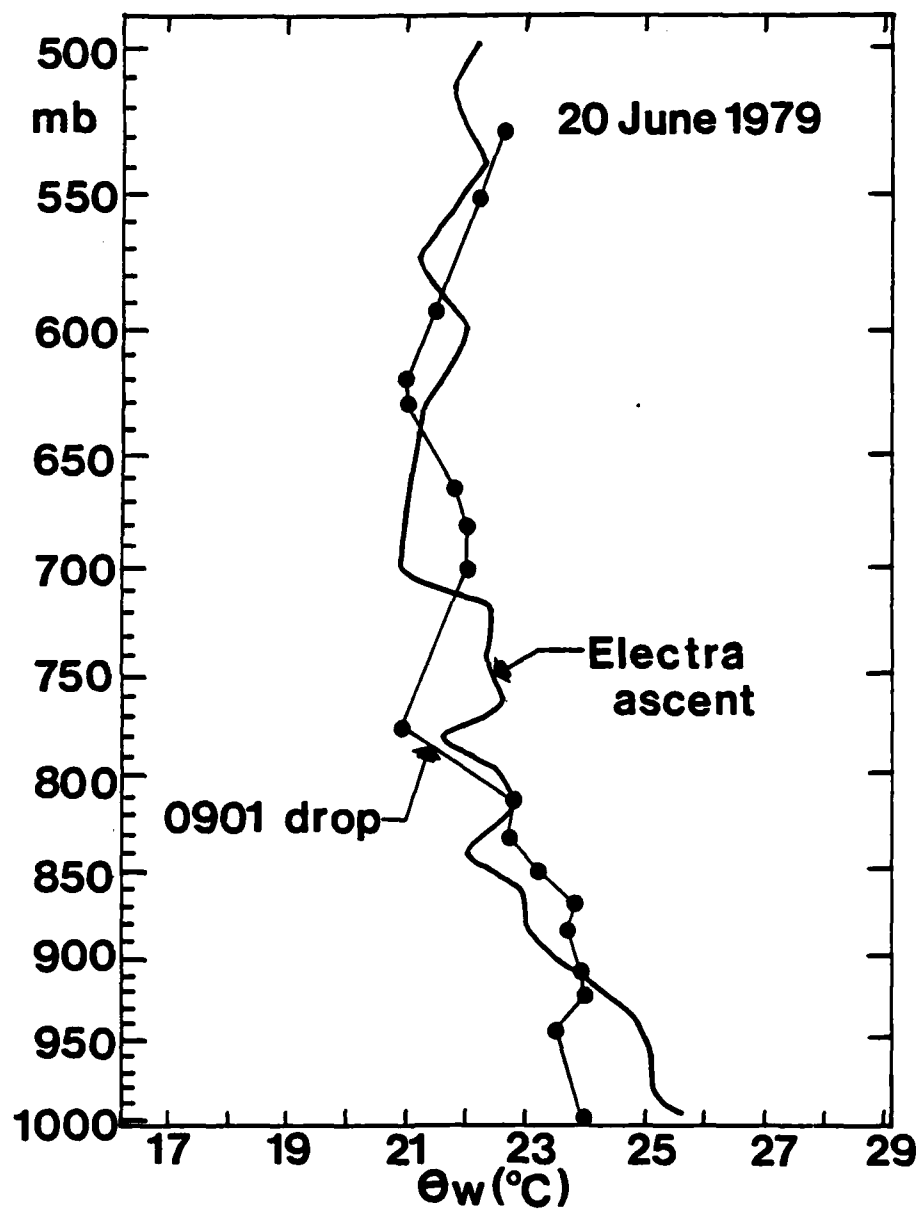


Fig. 30 Computed profiles of wet-bulb potential temperature (θ_w) for DWS #4 (0901 GMT) and ascent sounding on 20 June 1979.

lowest over-water θ_w found on 20 June 1979 at 1000 mb. The observed temperature of 25.0°C at 1000 mb in the 0901 GMT data was about 4.0°C cooler than the corresponding ascent sounding temperature. The low θ_w value of 24.0°C at 1000 mb apparently had its origin from around 915 mb in the pre-storm environment. Thus, this convective-scale downdraft had its origin slightly higher up in the lower troposphere than the downdraft pertaining to the mesoscale blob. It is consistent in the respect that the convective-scale downdraft origin was in the very low troposphere (i.e., from near or above the cloud base, not in the mid-troposphere). Computed θ_v profiles (not shown) suggest a virtual disappearance of the mixed layer in the 0901 GMT DWS data. The 0901 θ_w profiles showed no evidence of mesoscale subsidence. This is likely due to the fact that (1) the sounding was not taken under the anvil region, and (2) the convective area was clearly not a squall line.

d. Squall line influences at Amini

The squall line observed during the Electra's flight appears to have weakened by 0900 GMT. Since the Electra and AVRO research aircraft terminated their missions by 1000 GMT, the discussion in this section is based on satellite photos and island rawinsonde and surface data. By 1200 GMT a new squall line had formed just north of station Amini (11.1°N, 72.7°E; see Fig. 1). The squall line was clearly evident on 1200 GMT GOES-1 infrared

imagery (Fig. 6). This squall line was oriented along about a 240° - 060° axis, and appeared to be quasi-stationary before dissipating by 1800 GMT. The squall line at 1200 GMT, based on colder infrared temperatures, appears to have been ~650 km long. Although aircraft DWS soundings were not available from the vicinity of this squall line, a sounding was available from Amini at 1200 GMT. Amini's 1200 GMT θ_w profile is plotted with the 0524 GMT DWS θ_w profile (pre-squall sounding) in Fig. 31. The θ_w profile from Amini reveals that a relatively deep layer of low θ_w air has incurred below 905 mb, above which very high θ_w values are found to 842 mb. The ~1 km thick layer of low θ_w air in the BL is likely due to cooler and drier (in the sense that specific humidity is less) air from convective-scale downdrafts replacing the high energy θ_w air from before the squall line (Nicholls and Johnson, 1984).

Contrary to the DWS data, the Amini sounding data have surface observations to corroborate inferences from the computed θ_w profiles. The 0600, 1200, and 1800 surface temperature, dew point, wind direction and velocity, present weather, and sea-level pressure are reproduced in Table 1. The substantial temperature and dew point decrease, along with a windshift and dramatic increase in windspeed (between 0600 and 1200 GMT) is most unusual. Mean surface temperature and dew point values for June 1979 at Amini (not shown) show near constant values of temperature and dew point between 0600 and 1200 GMT. Mean values of

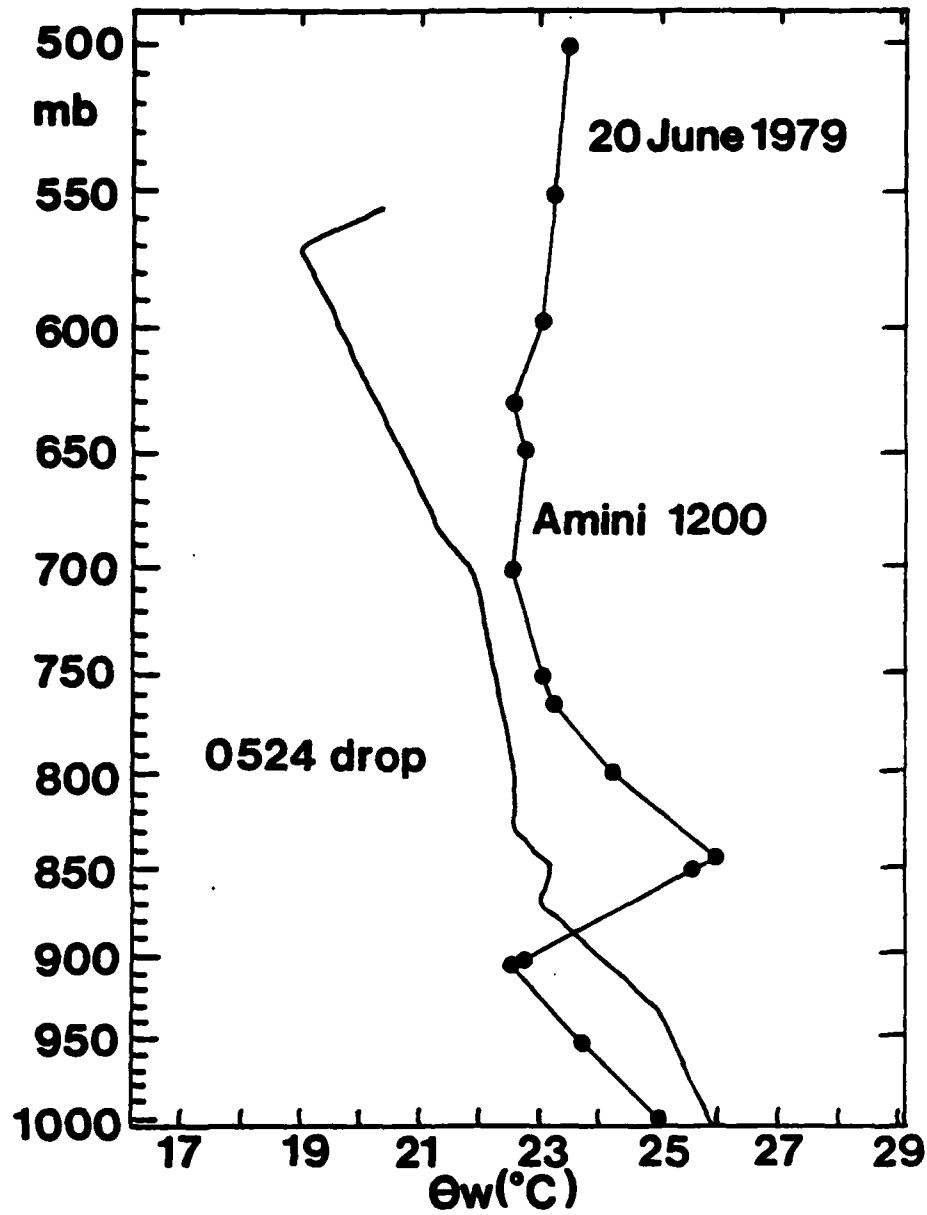


Fig. 31 Computed profiles of wet-bulb potential temperature (θ_w) for station Amini (1200 GMT) and DWS #3 (0524 GMT) on 20 June 1979.

surface wind between 0600 and 1200 GMT show an increase of 2.1 m s^{-1} , far less than the 10 m s^{-1} increase observed on 20 June.

Table 1. Surface weather elements observed at Amini (11.1°N , 72.7°E) on 20 June 1979.

Time (GMT)	T ($^{\circ}\text{C}$)	Td ($^{\circ}\text{C}$)	ddd (deg)	ff (m s^{-1})	Pressure (mb)	Present weather
0600	29.0	26.0	270	03	1010	—
1200	27.0	25.0	315	13	1007	☁
1800	26.6	25.4	315	14	1009	☁

The observed surface winds deserve further comment. The mean 1200 GMT surface winds for June 1979 at Amini were 265° at 7.5 m s^{-1} . Surface winds with a northwesterly direction at 1200 GMT were reported on only five other days, but in all five cases, speeds were 6 m s^{-1} or less. The mean 1800 GMT surface winds were 263° at 7.2 m s^{-1} . Surface winds north of 270° were reported at 1800 GMT on only two other days, and on these days the speeds were only 3 and 2 m s^{-1} . The causative mechanism for such anomalous surface winds and colder temperatures between 1200 and 1800 GMT could not be caused by some extratropical-type front; there was little synoptic scale variability of the tropical air mass over the eastern Arabian Sea on 20 June 1979. The only plausible explanation is that Amini was under the continuing

influence of outflow from convective scale downdrafts originating from the squall line some 45 km to the northwest. Since the outflow was coming over Amini from the northwest, this suggests that the outflow boundaries from the squall line could initiate convection further to the south and to the east. Indeed, satellite photos showed a band of new convection forming along $\sim 10.5^{\circ}\text{N}$ (just south of Amini) by 1800 GMT. The outflow boundary as a initiator of GATE convection has been documented by Leary and Houze (1979). The precipitation generation they described was favored by the precipitating cells being aligned perpendicular to the low level wind. No such arrangement is evident in this case, in fact satellite photos and aircraft reports clearly show the convection aligned parallel to the low-level flow. This may be why the convective bands observed at 1200 GMT infrared satellite imagery appeared as a north-south array of bands, separated by 50-100 km. At 1200 GMT, the band lengths increased going southward. A conceptual model of Arabian Sea squall lines will be presented in Chapter 5, pointing out the differences between Arabian Sea squall line development and the intensively studied GATE convection.

a. Measured vertical velocity events

Quantitative measurements of vertical velocity (w wind component) were available from data recorded at 20 s^{-1} using the Electra's gust probe. The magnetic tape containing the processed

data was obtained from NCAR. Vertical velocities were extracted from a 30 minute section of the tape (0447-0517 GMT). During this time the Electra was flying at a constant pressure level of 504 mb. The flight leg sampled is highlighted on the 0600 GMT GOES-I imagery (Fig. 32). Thus, quantitative assessment of updraft/downdraft strength for a portion of the convective cloud cluster is possible.

An updraft (downdraft) was defined as continuously positive (negative) vertical velocity measurements of $>0.5 \text{ m s}^{-1}$ for 500 m of flight. Since the Electra's airspeed was $\sim 140 \text{ m s}^{-1}$ during the sampled time period, $\sim 3.5 \text{ s}$ of upward (downward) vertical velocities exceeding 0.5 m s^{-1} would define an updraft (downdraft). An updraft (downdraft) core is defined as a region of continuously positive (negative) vertical velocities with an absolute magnitude greater than 1 m s^{-1} for $>500 \text{ m}$. The definition of updrafts and downdrafts is similar to, but not identical to LeMone and Zipser's (1980) definitions of vertical velocity events observed in GATE. (Specifics of the difference in updraft/downdraft definitions are discussed in the Appendix). The definition of updraft and downdraft cores however, is identical to LeMone and Zipser's definitions. Apparent from the definitions is the fact that all updraft and downdraft cores must be contained in updrafts and downdrafts. Not all updrafts and downdrafts contained cores, however. Mean updraft or downdraft vertical velocities (\bar{W}) for an individual updraft or downdraft



Fig. 32 GOES-I visual imagery for 0600 GMT 20 June 1979. The small hatch marks indicate the portion of the Electra flight path (at ~504 mb) from which vertical velocities were examined.

were computed using the formula:

$$\bar{w} = \frac{1}{N} \sum_{i=1}^N w_i \quad (4)$$

where \bar{w} is the mean updraft or downdraft vertical velocity; N is the number of vertical velocity measurements in an updraft or downdraft event; and w_i is the individual vertical velocity measurement. N varied depending on the size of the updraft or downdraft event, but averaged about 135 for updrafts and 120 for downdrafts.

Examination of the w measurements revealed 13 updrafts (1 of which contained an updraft core) and 4 downdrafts (3 of which contained downdraft cores). A listing of updraft and downdraft number, mean vertical velocity (\bar{w}), the instantaneous maximum or minimum vertical velocity ($|w_i|_{\max}$), and diameters are presented in Tables 2 and 3 for updrafts and downdrafts, respectively. The most obvious result of comparing the tables is the fact that updrafts at 504 mb greatly outnumbered downdrafts. Another obvious difference is that updraft diameter is greater than downdraft diameter in the mid-troposphere. Downdraft cores were also much stronger than updraft cores (although the small number of updraft and downdraft cores precludes any meaningful comparisons). Instantaneous updraft velocities ($|w_i|_{\max}$) varied from 0.67 to 2.62 m s^{-1} . Shin and Mak (1983) analyzed vertical velocities over the central Arabian Sea in a convective area on 16 June 1979. They found that "...updrafts with magnitudes of 1-3 m s^{-1}

Table 2. Updraft data as measured by the Electra's gust probe from 0447-0517 GMT on 20 June 1979. Measurements were made at constant flight level of 504 mb.

Updraft #	\bar{w} (m s ⁻¹)	$ w_{\perp} _{\max}$ (m s ⁻¹)	Diameter (m)	Contains core?
1	0.58	0.67	784	NO
2	0.97	2.04	518	NO
3	1.31	2.62	1232	NO
4	1.14	1.83	910	YES
5	1.01	1.74	868	NO
6	0.60	0.72	630	NO
7	0.72	0.95	1106	NO
8	0.75	0.97	1000	NO
9	0.69	0.81	1260	NO
10	0.76	1.07	1764	NO
11	0.73	1.01	924	NO
12	0.61	0.78	546	NO
13	0.73	0.95	672	NO

are common " (p. 1589). However they stated no objective criteria for defining updrafts or downdrafts.

Table 3. Same as Table 2, but for downdraft measurements. ($|w_1|_{\max}$ for this data implies maximum downward vertical velocities.)

Downdraft #	\bar{w} (m s^{-1})	$ w_1 _{\max}$ (m s^{-1})	Diameter (m)	Contains core?
1	-0.89	1.37	1036	No
2	-2.30	4.20	575	Yes
3	-2.10	4.04	910	Yes
4	-0.97	1.92	602	No

The median updraft velocity of 0.74 m s^{-1} in this study is very close to LeMone and Zipser's (1980) median w of $\sim 0.75 \text{ m s}^{-1}$ for updrafts encountered at altitudes of 4300-8100 m during 6 days of GATE data. Their median updraft diameter of $\sim 1.05 \text{ km}$ compares favorably with our median diameter of $\sim 940 \text{ m}$.

The vertical velocity measurements can be examined in relation to one DWS sounding (0449 GMT). The profile for this sounding (Fig. 19) strongly suggests that modification of the near surface layers came from the lower troposphere (around 892 mb). All vertical velocity values between 0447 and 0449 GMT were examined, and no negative values were found: this supports the contention that the downdrafts could not have originated in the

mid-troposphere.

Temperature data recorded at 20 s^{-1} were matched with simultaneous vertical velocity values to determine how warm (or cold) updrafts (or downdrafts) were in relation to their immediate environment. After the data were compared, an apparent negative correlation became evident between w and T . Shin and Mak (1983) obtained similar results in their analysis of 16 June 1979 temperature and vertical velocity data. They concluded that this apparently unreal physical relationship was likely due to erroneous readings by the temperature sensor due to wetting by cloud droplets and rain. They cautioned that "...analysts of MONEX aircraft data should exercise great care in making interpretation of the temperature related results." Thus, no further attempt to relate mid-tropospheric temperatures and vertical velocities was made in this study.

5. SUMMARY AND CONCLUSIONS

a. Summary of research

Squall lines are powerful energy exchangers in the tropics, especially in the vertical (Barnes and Garstang, 1982). Over the eastern Arabian Sea, squall lines embedded in convective cloud clusters can exist for several days, particularly after the establishment of the southwest monsoon. They were studied earlier by Bunker and Chaffee (1969), and were summarized by Rao (1976). A unique opportunity to study a squall system over the eastern Arabian Sea was afforded on 20 June 1979 as the MONEX-79 research aircraft penetrated the system and provided in situ measurements. In addition, the GOES-I visual and IR imagery available at ~3 h intervals provided a graphical depiction of the temporal variation of the cloud structure.

Briefly speaking, an area of active convection $\sim 1.2 \times 10^6$ km² became organized on 19 June 1979 over the northeastern Arabian Sea. Consolidation took place during 20 June (up to about 1200 GMT) near 14°N, 72°E. After 1200 GMT the synoptic scale convective cloud cluster became disorganized to the point that it could not be described as a discrete weather system by 2300 GMT.

Rainfall estimates associated with the cloud cluster on 20 June exceeded 120 mm over the extreme eastern Arabian Sea (Krishnamurti et al., 1983) near 16°N, 72°E. A secondary maxima exceeding 80 mm was centered near 11.5°N, 75.0°E. This point was centered over the area affected by the squall line that formed north of Amini at around 1200 GMT.

On the synoptic scale, the parent cluster featured a highly convergent westerly flow in the BL. Peak speeds of $\sim 25 \text{ m s}^{-1}$ were found in the 900-850 mb layer associated with a branch of the Somalia Jet. A monotonic decrease in the westerly flow was observed above this level up to ~ 500 mb. The BL's static energy increased from west to east across the eastern Arabian Sea as the flow was gradually warmed and moistened by slowly increasing sea-surface temperatures.

Above 500 mb, the flow became easterly and continued to increase to the ~ 150 mb level. The upper-tropospheric flow was dominated by the TEJ. The TEJ had two distinct functions in the life of the cluster and its component convection. First, convergent/divergent aspects of the TEJ at 200 mb (cirrus outflow level) could act to either enhance convection (divergent flow) or inhibit convection (convergent flow). Secondly, the TEJ was crucial to the convective development because it determined the orientation and direction of the anvil cloud (that was most prominent in squall line convection). Satellite imagery indicated that cirrus blowoff from squall line convection could extend ~ 600

AD-A157 973

SQUALL AND CLOUD LINES AS STRUCTURAL COMPONENTS OF AN
ARABIAN SEA CONVECTIVE CLOUD CLUSTER(U) AIR FORCE INST
OF TECH WRIGHT-PATTERSON AFB OH C L BENSON 1985
AFIT/CI/NR-85-83T

2/2

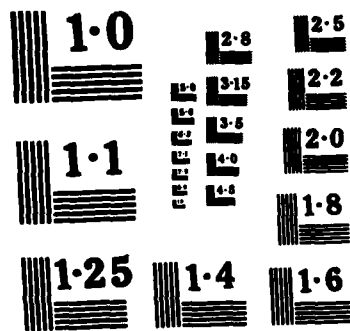
UNCLASSIFIED

F/G 4/2

NL



			END
			PAVED
			OTC



NATIONAL BUREAU OF STANDARDS
MICROCOPY RESOLUTION TEST CHART

km downwind from the active convection. However, only a small portion of this distance could be classified as thick anvil cloud. The anvil discouraged new convective growth by developing subsidence beneath its base (~500 mb) down to about 800 mb. The 900-850 mb jet may have inhibited sinking below this level.

Although a number of convective types (squall lines, mesoscale convective blobs, cloud lines, etc.) were observed on 20 June by research aircraft, the squall lines were probably the most important type observed. At least two squall lines were observed on 20 June. The first was encountered by the Electra at around 0526 GMT. The Electra passed through the ~25 km wide line of active convection at this time. A θ_w profile from a DWS release ahead of the line was distinctly different from the θ_w profile constructed from the sounding as the aircraft descended from the squall. Lower θ_w values were found up to 650 mb in the descent sounding. Substantial reductions in θ_w above 875 mb were likely the result of unsaturated downdrafts that formed beneath the trailing (and precipitating anvil cloud). This area sampled by the Electra to the southwest of the squall line (under the sheared anvil cloud) was characterized by subsidence (Warner, 1983). Meyer (1982) concluded that thermodynamically, this area resembled the "wake region" to the rear of precipitating convection. This region was thus unavailable for new convective development until the BL recovered to its normal thermodynamic structure. Tao (1984) estimates this process would take ~6 h.

This relatively rapid recovery time is primarily due to the strong surface winds observed over the region.

The other squall line observed in this research was observed by 1200 GMT satellite photos (IR), and by observations from station Amini. The Amini profile suggests the incursion of cool, moist air from the squall line some 40-50 km to the north. Concurrent with this incursion of low energy air below 900 mb was a wind shift from southwest to northwest with an increase in speed from 4 m s^{-1} to 13 m s^{-1} .

In summary, it appears that the convective-scale updrafts occurred along the northern edges of the squall lines. The updrafts were arranged WSW-ESE primarily due to the mesoscale convergence within the low-level flow. The low-level flow was also convergent on the synoptic scale. The convective scale downdrafts apparently originated just above the cloud base, but below the level of the 850 mb jet. Due to the strong westerly low-level flow, these downdrafts were able to travel horizontally ~50 km or more in an east-southeasterly direction. New convection was initiated when the cool boundary entered a region of high energy subcloud air. This method of propagation may be the reason the synoptic scale system appeared to drift to the southeast during 20 June: the component convection actually was reforming continuously to the south and east of older convection. Thus, the branch of the Somali jet (~850 mb) had two important functions: (1) its convergent characteristics initiated the deep con-

vection, and (2) its orientation tended to blow the cool convective-scale downdraft air mostly to the east-southeast.

The influence of the TEJ was just as important in the sustenance of the convective cloud cluster and its component squall lines as the low level jet, as mentioned previously in this section. Figs. 32 and 33 are conceptualized schematics of an eastern Arabian Sea squall line, showing the proposed interaction of the TEJ and the branch of the Somali jet. The interaction between the TEJ and the low-level jet appear to be explicit through convection. The convection is forcing the upper easterlies to curve either south-southwest or west-northwest. This phenomenon is promoting divergence aloft, which in time encourages convection. The low-level flow appears to aid new convective growth by participating in the updrafts on the northern side of individual convective bands. The low-level flow appears to influence new convective growth through a delayed action of transforming the cool, stable convective-scale downdraft air into a conditionally unstable state. The role of convective scale updrafts and downdrafts, as well as mesoscale downdrafts are also displayed in the conceptualized schematics.

b. Arabian Sea ya. GATE convection

Probably the most extensively studied tropical squall lines in recent history were those observed in GATE (House, 1977; Zipser, 1977; etc.). It is appropriate here to outline the main

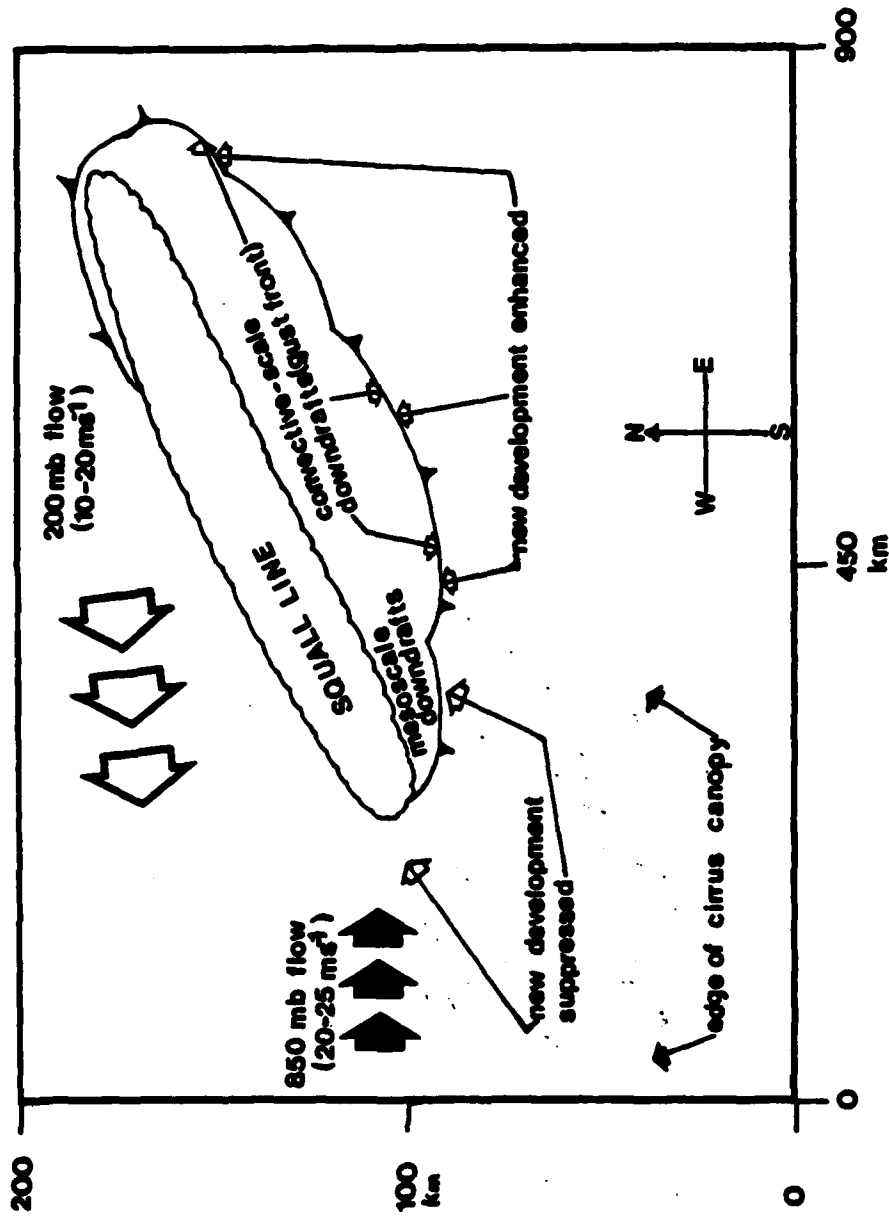


Fig. 33 Conceptual model (x-y plane) of the eastern Arabian Sea squall lines observed on 20 June 1979.

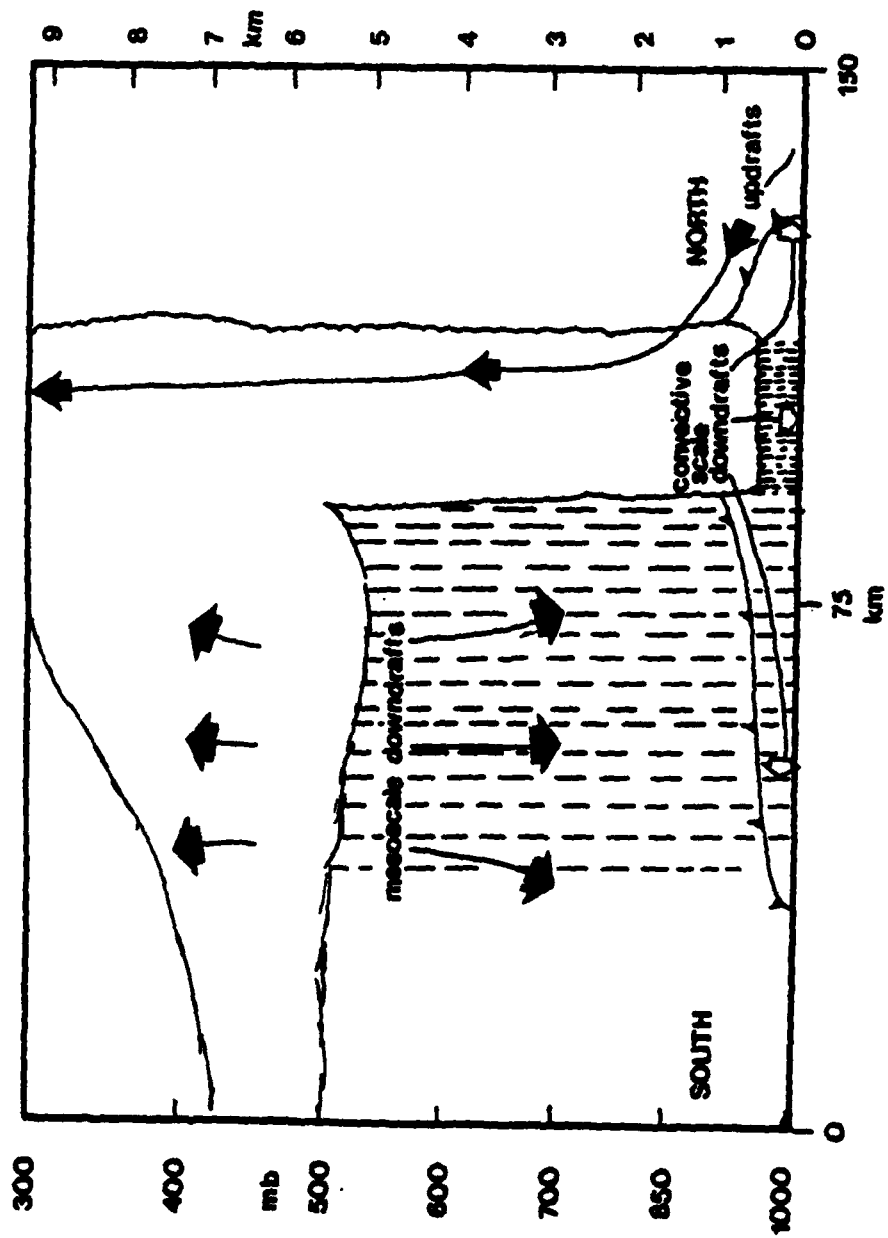


Fig. 34 Conceptual model (y-z plane) of the eastern Arabian Sea squall observed on 20 June 1979.

differences between Arabian Sea squall lines and those studied during GATE.

The most obvious difference in physical structure is the fact that the anvils in Arabian Sea squall lines can be sheared toward the west, back over the high energy low-level westerly flow (Grossman and Durran, 1982). In GATE, the high energy inflow was more or less "protected" from subsidence beneath the precipitating anvil cloud. The vertical shear in GATE was not intense.

The inflow energy air in Arabian squall lines was characterized by higher q_w values than GATE convection. This is likely a direct result of higher sea surface temperatures over the eastern Arabian Sea as compared to those observed in the eastern Tropical Atlantic Ocean during GATE.

Mixed layer depths in an undisturbed environment over the eastern Arabian Sea were significantly greater (650 m vs 500 m) than those observed during GATE. Substantial mixed layer depth suppression was observed in the immediate environment of precipitating convection, as found in GATE convection studies. Theoretically, recovery times for the mixed layer over the eastern Arabian Sea should be faster than recovery times in GATE. This is a direct consequence of the higher surface winds observed over the eastern Arabian Sea vis-a-vis GATE surface winds.

While the squall lines in GATE generally were moving (some as fast as 17 m s^{-1}), the squall lines observed in this study

were quasi-stationary. Although individual lines were quasi-stationary, new development appeared to occur to the south and east, resulting in apparent southeast translation of the convective cloud cluster's component convection.

The last major difference is the fact that Arabian Sea squall lines appeared to form parallel to the low-level flow. A number of GATE studies (Leary and Houze, 1979a) indicated that new squall line formation was favored perpendicular to the low-level flow.

a. Conclusions

Distinct squall lines were observed in a convective cloud cluster over the eastern Arabian Sea on 20 June 1979. Other types of convection were observed, but the squall lines were the most important. All types of precipitating convection observed modified the maritime BL. These BL modifications are important in convective development over the eastern Arabian Sea during the Indian southwest monsoon. The evolution of deep convection during the monsoon is the result of a complex interaction of synoptic-scale features such as the TEJ, and the 850 mb-Somalia jet, as well as features on the mesoscale such as anvil influences, mesoscale wind speed variability, and the downdraft air spreading horizontally. The aforementioned BL transformations are important, and cannot be ignored in attempting to depict (either descriptively or numerically) the Indian southwest

monsoonal rainfall, particularly near the west coast.

APPENDIX

DEFINITIONS OF VERTICAL VELOCITY EVENTS

(UPDRAFTS AND DOWNDRAFTS)

Using the Electra's gust probe data (sample rate of 20 s^{-1}), an updraft (downdraft) was defined as a flight leg of at least 500 m in length where instantaneous vertical velocity (w_1) measurements were continuously positive (negative), with absolute values greater than 0.5 m s^{-1} (i.e., for each w_1 , $w_1 > 0.5 \text{ m s}^{-1}$). So, w_1 would be positive for updrafts, negative for downdrafts.

This definition is not identical to LeMone and Zipser's (1980) definitions for GATE vertical velocity events. They defined updrafts (downdrafts) as a flight leg of at least 500 m in length characterized by vertical velocity measurements (w_1) continuously greater than zero (updraft) or less than zero (downdraft); and $w_1 > 0.5 \text{ m s}^{-1}$ for at least 150 m (i.e., for updrafts $w_1 > 0$ for 500 m, and $w_1 > 0.5 \text{ m s}^{-1}$ for at least 150 m).

LeMone and Zipser's definition is not suitable for this study. This is because the aircraft intercepted extensive areas where small positive w_1 values were obtained. If such a large

area was adjacent to an area where $w_1 > 0.5 \text{ m s}^{-1}$ for 150 m s^{-1} , then an updraft would be diagnosed with a width of many kilometers. Thus, invoking the more stringent requirement that $w_1 > 0.5 \text{ m s}^{-1}$ continuously for 500 m leads to results that are more physically reasonable.

BIBLIOGRAPHY

- Agarwal, O. P., and G. Krishnamurti, 1967: A radar study of line-type thunderstorms over Bombay airport and surroundings. Indian J. Meteor. and Geophysics, 19, 35-40.
- Barnes, G. M. and M. Garstang, 1982: Subcloud layer energetics of precipitating convection. Mon. Wea. Rev., 110, 102-117.
- Betts, A. K., 1976: The thermodynamic transformation of the tropical subcloud layer by precipitation and downdrafts. J. Atmos. Sci., 33, 1008-1020.
- _____, R. W. Grover, and M. W. Moncrieff, 1976: Structure and motion of tropical squall-lines over Venezuela. Quart. J. Roy. Meteor. Soc., 102, 395-404.
- Bhumralker, C. M., 1978: Relationship between evaporation over the Arabian Sea and rainfall at the west coast of India during the summer monsoon. Indian J. Meteor. and Geophysics, 29, 150-161.
- Bolhofer, W. C., M. Chambers, D. Frey, J. P. Kuettnner, and S. Unninayer, 1981: Summer MONEX U. S. research flight missions, May-July 1979. NCAR/TN-168+STR, 167 pp.
- Bunker, A. F., and M. Chaffee, 1969: Tropical Indian Ocean clouds. Met. Monograph No. 4, University of Hawaii, Honolulu.
- Colon, Jose, A., 1964: On interactions between the Southwest Monsoon Current and the sea surface over the Arabian Sea. Indian J. Meteor. and Geophysics, 15, 183-200.
- Desai, B. N., N. Rangachari, and S. K. Subramanian, 1976: Structure of low-level jet-stream over the Arabian Sea and the Peninsula as revealed by observations in June and July during the monsoon experiment (MONEX) 1973 and its probable origin. Indian J. Meteor. and Geophysics, 27, 261-274.
- Fitzjarrald, D. R., and M. Garstang, 1981a: Vertical structure of the tropical boundary layer. Mon. Wea. Rev., 109, 1512-1526.
- _____, and _____, 1981b: Boundary-layer growth over the tropical ocean. Mon. Wea. Rev., 109, 1762-

1772.

- Fleagle, R. G., J. A. Businger, 1980. An Introduction to Atmospheric Physics. Academic Press, 432 pp.
- Gamache, J. F., and R. A. Houze, Jr., 1982: Mesoscale air motions associated with a tropical squall line. Mon. Wea. Rev., 110, 118-135.
- Grossman, R. L., and D. R. Durran, 1984: Interaction of low-level flow with the Western Ghat Mountains and offshore convection in the summer monsoon. Mon. Wea. Rev., 112, 652-672.
- Haltiner, G. J., and R. T. Williams, 1980: Numerical Prediction and Dynamic Meteorology. John Wiley and Sons, 477 pp.
- Hamilton, R. A., and J. W. Archbold, 1945: Meteorology of Nigeria and adjacent territory. Quart. J. Roy. Meteor. Soc., 71, 231-262.
- Holton, R., 1979: An Introduction To Dynamic Meteorology. Academic Press, 319 pp.
- Houze, R. A., Jr., 1977: Structure and dynamics of a tropical squall-line system. Mon. Wea. Rev., 105, 1540-1567.
- Jambunathan, R., and K. Ramamurthy, 1974: Wind field in the lower and middle troposphere over the Arabian Sea during the southwest monsoon 1973. Indian J. Meteor. and Geophysics, 25, 403-410.
- Johnson, R. H., and M. E. Nicholls, 1983: A composite analysis of the boundary layer accompanying a tropical squall line. Mon. Wea. Rev., 111, 308-319.
- Krishnamurti, T. N., P. Ardanuy, Y. Ramanathan, and R. Pasch, 1979: Quick-look 'Summer MONEX Atlas', Part II - The Onset Phase. Florida State University, FSU Report 79-5, 205 pp.
- _____, S. Cocke, R. Pasch, and S. Lownam, 1983: Precipitation estimates from raingauge and satellite observations summer MONEX. FSU Report No. 83-7, 373 pp.
- Leary, C. A., and R. A. Houze, Jr., 1979a: The structure and evolution of convection in a tropical cloud cluster. J. Atmos. Sci., 36, 437-457.
- _____, and _____, 1979b: Melting and evaporation of hydrometeors in precipitation from the anvil clouds of deep tropical convection. J. Atmos. Sci., 36, 669-679.

- LeMone, M. A., and E. J. Zipser, 1980: Cumulonimbus vertical velocity events in GATE. Part I: Diameter, intensity, and mass flux. J. Atmos. Sci., 37, 2444-2457.
- Mansfield, D. A., 1977: Squall lines observed in GATE. Quart. J. Roy. Meteor. Soc., 102, 569-574.
- Meyer, W. D., 1982: An analysis of the monsoon boundary layer over the Arabian Sea employing fast-response aerial turbulence data. Ph.D. dissertation, Department of Earth and Atmospheric Sciences, Saint Louis University, 199 pp.
- Miller, M. J., and A. K. Betts, 1977: Traveling convective storms over Venezuela. Mon. Wea. Rev., 105, 833-848.
- Moncrief, M. W., and M. J. Miller, 1976: The dynamics and simulation of tropical cumulonimbus and squall lines. Quart. J. Roy. Meteor. Soc., 102, 373-394.
- Nicholls, M. E., and R. H. Johnson, 1984: A model of a tropical squall line boundary layer wake. J. Atmos. Sci., 41, 2774-2792.
- Pant, M. C., 1978: Vertical structure of the planetary boundary layer in the west Indian Ocean during the Summer Monsoon as revealed by ISMEX data. Indian J. Meteor. and Geophysics, 29, 88-98.
- Ramage, C. S., 1971: Monsoon Meteorology. Academic Press, 296 pp.
- Rao, Y. P., 1976: The Southwest Monsoon. Indian Meteorological Department Monograph, Synoptic Meteorology 1/1976. Indian Meteorological Department, 367 pp.
- Riehl, H., 1979: Climate and Weather in the Tropics. Academic Press, 611 pp.
- Shin, K. S., and M. Mak, 1983: Aircraft measurements of the subsynoptic scale properties of the monsoonal onset-vortex of 1979. Mon. Wea. Rev., 111, 1587-1598.
- Smith, C. L., E. J. Zipser, S. M. Daggupati, and L. Sapp, 1975: An experiment in tropical mesoscale analysis: Part I. Mon. Wea. Rev., 103, 878-892.
- Soundra Rajan, K., 1960: Squalls at Bangalore. Indian J. Meteor. and Geophysics, 11, 583-589.
- Tao, C. R., 1984: A study of the various marine boundary layers - barotropic, baroclinic, suppressed and recovered. M.S.

thesis, Saint Louis University, 75 pp.

Wallace, J. M., and P. V. Hobbs, 1977: Atmospheric Science-An Introductory Survey. Academic Press, 467 pp.

Warner, C., 1983: Cloud maps for 20 June 1979 over the Arabian Sea: summer MONEX. University of Virginia Report, 10 pp.

Zipser, E. J., 1969: The role of organized unsaturated convective downdrafts in the structure and rapid decay of an equatorial disturbance. J. Appl. Meteor., 8, 799-814.

_____, 1977: Mesoscale and convective-scale downdrafts as distinct components of squall-line structure. Mon. Wea. Rev., 105, 1568-1589.

_____, and C. Gautier, 1978: Mesoscale events within a GATE tropical depression. Mon. Wea. Rev., 106, 789-805.

VITA AUCTORIS

The author, Charles Loren Benson, Jr., was born on November 12, 1955, in Lubbock, Texas. His family moved to Houston, Texas in 1965. There he attended Westchester Senior High School from 1969-1973. The author entered Texas A&M University in the fall of 1973. He graduated from Texas A&M with a Bachelor of Science degree (meteorology) in the spring of 1977.

The author was commissioned as an officer in the United States Air Force on August 15, 1978. He was subsequently assigned as a meteorologist to Dyess AFB (Abilene), Texas. In the spring of 1981 the author was assigned to Kunsan Air Base, Republic of Korea, as a meteorologist. In the spring of 1982 he was assigned to Scott AFB, Illinois as the executive assistant to the Air Weather Service commander. In January, 1984 he began a program at Saint Louis University leading to a Master of Science (Research) degree in meteorology.

The author is married to the former Lisa Anne Dowdy and has an infant daughter, Christine Anne. The author and his wife are active members of Zion Lutheran Church (Missouri Synod) in Mascoutah, Illinois.

END

FILMED

10-85

DTIC